

## Target-Related Applications of First Principles Quantum Chemical Methods in Drug Design

Andrea Cavalli,<sup>†</sup> Paolo Carloni,<sup>‡</sup> and Maurizio Recanatini<sup>\*†</sup>

Department of Pharmaceutical Sciences, University of Bologna, Via Belmeloro 6, I-40126 Bologna, Italy, and International School for Advanced Studies, SISSA, and INFN-DEMOCRITOS Modeling Center for Research in Atomistic Simulation, Via Beirut 2-4, 34014 Trieste, Italy

Received January 16, 2006

### Contents

1. Introduction	3497
2. Theoretical Methods	3500
3. Target-Based Applications of QM Methods	3501
3.1. Enzymes	3501
3.1.1. Selected Proteases	3502
3.1.2. Penicillin-Binding Proteins (PBPs) and $\beta$ -Lactamases	3508
3.1.3. Dihydrofolate Reductase	3511
3.2. Receptors and Channels	3512
3.2.1. Receptors	3512
3.2.2. Ion Channels	3513
4. Conclusions and Outlook	3514
5. Abbreviations	3515
6. Acknowledgments	3516
7. References	3516

### 1. Introduction

A fundamental postulate in the classical drug design paradigm is that the effect of a drug in the human body is a consequence of the molecular recognition between a ligand (the drug) and a macromolecule (the target). The pharmacological activity of the ligand at its site of action is ultimately due to the spatial arrangement and electronic nature of its atoms, and the way these atoms interact with the biological counterpart.<sup>1</sup>

Computational chemistry tools allow one to characterize the structure, dynamics, and energetics of such interactions. For instance, molecular mechanics (MM)-based approaches can efficiently assist the discovery of new drug candidates, and these computationally inexpensive methods are nowadays routinely used in drug design.<sup>2</sup> However, if a description of the electronic properties is deemed necessary, there is no

substitute for quantum mechanics (QM). Indeed, since QM-based approaches also account for quantum electronic effects, they describe bonds forming/breaking, polarization effects, charge transfer, etc., and usually estimate molecular energies more accurately.<sup>3</sup>

Historically, ligand-based applications of QM in drug design were devoted to investigations of energy, geometry, and electronic features (e.g., HOMO, LUMO, dipole moment, etc.) of small organic molecules (for a review, see refs 4 and 5). QM calculations mainly carried out at the semiempirical level<sup>6,7</sup> have also been routinely used in classical QSAR<sup>8,9</sup> and 3D QSAR<sup>10,11</sup> analyses and in developing quantum descriptors<sup>12,13</sup> to be used in the investigation of structure–activity correlations. The molecular quantum similarity method developed in 1995 by Carbo et al.<sup>14</sup> represents a key contribution in this respect.<sup>15</sup> Target-related applications of QM-based computations are nowadays used to unravel issues in which classical MM approaches may partially or fully fail. This is the case, for example, with metalloprotein active sites, where MM force fields must be ad hoc parametrized to properly account for metal coordination complexes.<sup>16,17</sup> Another field of target-related QM applications is represented by computational studies on ion channels, which are of crucial importance in contemporary biological and medicinal chemistry. Here, large electric fields responsible for the permeation of ions ( $K^+$ ,  $Ca^{2+}$ ,  $Cl^-$ ,  $Na^+$ , etc.) and possible charge-transfer effects demand QM tools to describe the physicochemical events occurring in the lumen of the channel. QM methods are also fundamental to studying biological reactions, as quantum electronic effects must be taken into account to properly describe the phenomena of bonds forming/breaking. Of particular interest among target-related applications of QM methods in drug design<sup>18</sup> is the study of enzymatic reactions carried out by biological systems of pharmacological relevance, as these simulations allow one to describe the mechanism of the substrate (inhibitor)–enzyme reaction and finally to capture the substrate–enzyme interactions at the transition state (TS) configuration.<sup>19</sup> These features can then be exploited to address the rational design of potent TS analogues.<sup>20,21</sup> In this

\* Corresponding author. E-mail: maurizio.recanatini@unibo.it. Phone/Fax: +39 051 2099720/34.

<sup>†</sup> University of Bologna.

<sup>‡</sup> International School for Advanced Studies, SISSA, and INFN-DEMOCRITOS Modeling Center for Research in Atomistic Simulation.



Andrea Cavalli received his degree in Medicinal Chemistry in 1996 from the University of Bologna (Italy). In 1999, he received his Ph.D. degree in Pharmaceutical Sciences from the same university, under the supervision of Maurizio Recanatini. He was then a postdoctoral fellow in Biophysics at the International School for Advanced Studies (SISSA/ISAS) of Trieste (Italy), where he worked with Vincent Torre and Paolo Carloni. In 2001/2002, he was Visiting Scientist at the Swiss Federal Institute of Technology (ETH) of Zürich (Switzerland), working with Gerd Folkers and Leonardo Scapozza. At present, he is Assistant Professor of Medicinal Chemistry at the Department of Pharmaceutical Sciences at the University of Bologna. His research interests are focused on the development and application of computational methods in drug design. In 2003, he was awarded the Farmindustria Prize for Pharmaceutical Research.

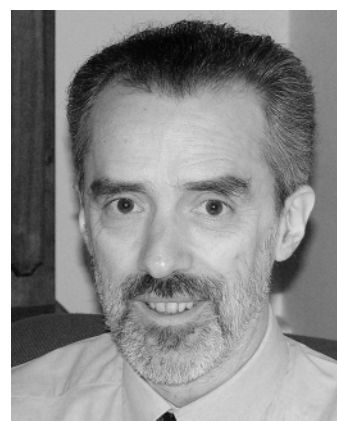
context, these calculations can also be used to investigate the action of prodrugs<sup>22</sup> or suicide substrates<sup>23</sup> reacting with enzymatic systems. Finally, QM methods can be used to investigate chemical structures, charge distributions, and energetics, which may be useful for developing MM force fields.

QM methods can be divided into two main categories: (i) those based on empirical parametrizations (semiempirical methods), which perform best for systems for which much experimental information is known and which might be considered computationally inexpensive, and (ii) those solely based on the QM laws (first principles methods), without reference to experimental data. Even though, in some specific cases, it has been argued that AM1 binding enthalpies show a good correlation with those computed at the MP2 level of theory,<sup>24</sup> first principles methods may be better suited to dealing with drugs, because of their enormous structural diversity. However, first-principles-based calculations may be very demanding from a computational point of view. In this respect, density functional theory (DFT)<sup>25</sup> has radically changed the scenario, opening the way for more computationally affordable yet accurate descriptions of the electronic structure of the matter, and indeed DFT-based applications in drug design are appearing in the literature at an increasing pace.<sup>26,27</sup> Gradient-corrected DFT calculations include electron correlation effects neglected in the Hartree–Fock theory at a similar computational cost, although they do encounter difficulties in describing London dispersion forces, which are crucial interactions in drug–target complexes. However, very promising approaches may soon be able to overcome this drawback.<sup>28,29</sup>

Since most living organisms work at about 310 K, the possibility of simulating biological systems by means of molecular dynamics (MD) simulations<sup>30,31</sup> adds substantial value when studying complex phenomena by means of currently available QM methods. In the DFT framework, first principles MD was originally developed in 1985 and implemented in the Car–Parrinello molecular dynamics (CPMD) method.<sup>32</sup> This approach allows one to carry out



Paolo Carloni obtained his Ph.D. at the University of Firenze (Italy) under the supervision of Michele Parrinello, Lucia Banci, and Pierluigi Orioli in 1993. Since 1998, he has been Professor of Chemistry at the International School for Advanced Studies, in Trieste (Italy). He is also responsible for the Biophysics line of research of the INFN-CNR DEMOCRITOS Center for Atomistic Simulation. For more than 15 years, his main interest has been the molecular simulation of systems of biological relevance.



Maurizio Recanatini received his degree in Chemistry from the University of Bologna (Italy) in 1978. He worked as a postdoctoral fellow until 1983, when he joined the Faculty of Pharmacy at the same university. In 1984–85, he was a Visiting Scientist at the Department of Chemistry of the Pomona College, Claremont, CA (USA) in the laboratory of Corwin Hansch. Since 2000, he has been Full Professor of Medicinal Chemistry at the University of Bologna, carrying out his research at the Department of Pharmaceutical Sciences. His research interests are focused on the application of computational methods to drug design and discovery.

MD simulations, with the potential energy on the systems being computed at the DFT level of theory. Finally, the development of mixed QM/MM schemes,<sup>33–35</sup> which enable the study of a protein active site at the QM level, while treating the rest of the protein and the solvent by means of classical MM force fields, has further expanded the scope of QM methods in general and DFT in particular. By taking into account tens of thousands of atoms, QM/MM-based computations allow simulations of protein targets in their physiological environment. In this respect, the recent implementation of the CPMD method into a QM/MM mixed code<sup>36–38</sup> provides a further way of simulating, at the QM level, macromolecular systems of pharmacological interest.

In this article, we review some recent applications of QM in drug design (covering approximately the last four years), focusing exclusively on target-based studies carried out on pharmacologically relevant protein systems. Rather than report all the literature in the field (a tentative comprehensive survey is reported in Tables 1 and 2), we wish to give the reader a flavor of how these techniques have been exploited

**Table 1. Survey (Covering Approximately the Last Four Years) of First Principles QM Applications to Therapeutically Relevant Enzymes**

protein family	target biological system	therapeutic area	QM method	studied feature	ref	
proteases	HIV-1 protease	anti-AIDS	DFT(CPMD)	effect of conformational fluctuations on the catalysis	85	
	HIV-1 protease	anti-AIDS	DFT	H-bond network	88	
	HIV-1 protease	anti-AIDS	AM1/MM	enzyme–inhibitor interactions	237	
	HIV-1 protease	anti-AIDS	DFT(CPMD)/MM	reaction mechanism	86	
	HIV-1 protease	anti-AIDS	HF	binding interaction of six FDA-approved drugs	238	
	HIV-1 protease	anti-AIDS	HF DFT	binding interaction of three inhibitors	96	
	HIV-1 protease	anti-AIDS	DFT(CPMD)/MM	active site H-bond network	239	
	serine protease	anticancers antiarthritis	HF/MM	stability of the tetrahedral intermediate during the deacylation reaction	132	
	serine protease	anticancers antiarthritis	DFT	rate-limiting step	240	
	serine protease	anticancers antiarthritis	MP2/MM	acylation reaction	98	
	serine protease	anticancers antiarthritis	HF/MM MP2/MM	entire catalytic cycle	100	
	serine protease	anticancers antiarthritis	DFT	His-Asp H-bond interaction	241	
	serine protease	anticancers antiarthritis	DFT/MM	His-Asp H-bond interaction on tetrahedral complex formation	242	
	serine protease	anticancers antiarthritis	HF/MM	role of Asp in the catalysis	131	
	serine protease	anticancers antiarthritis	DFT HF/MM	deacylation reaction	99	
	cysteine protease (caspase)	anticancers	DFT(CPMD)/MM	deacylation reaction	137	
	cysteine protease (caspase)	anti-Alzheimer anticancers	DFT	ring opening reactions of three-membered heterocycles	140	
	cholin-esterases	AChE	anti-Alzheimer	MP2/MM	initial step of the acylation reaction	113
		AChE	anti-Alzheimer	HF/MM	initial step of the acylation reaction	114
		AChE	anti-Alzheimer	DFT	initial step of the acylation reaction	243
AChE		anti-Alzheimer	DFT	fasciculin–AChE interactions	115	
BChE		anticocaine medication	QM/MM	H-bond network	244	
BChE		anticocaine medication	MP2/MM	mechanism of hydrolysis of cocaine	118	
$\beta$ -lactamases	$\beta$ -lactamase	antibacterials	HF	chemical reactivity differences between clavulanic and penicillanic acids	245	
	$\beta$ -lactamase	antibacterials	DFT	role of Lys73 and the substrate C3-carboxyl group in the deacylation step	246	
	$\beta$ -lactamase	antibacterials	HF	acylation reaction	147	
	$\beta$ -lactamase	antibacterials	AM1/MM	role of flexibility in the deacylation reaction	247	
	$\beta$ -lactamase	antibacterials	AM1/MM DFT/MM	determination of the reaction general base	149	
	$\beta$ -lactamase	antibacterials	DFT/MM	hydrolysis of acyl-enzyme intermediates	152	
	$\beta$ -lactamase	antibacterials	AM1/MM DFT/MM	mechanisms of antibiotic resistance	150	
	$\beta$ -lactamase	antibacterials	DFT	activation of Ser70 in the acylation	248	
	$\beta$ -lactamase	antibacterials	DFT/MM	carboxylation of lysine	249	
	$\beta$ -lactamase	antibacterials	MP2/MM	serine acyl-enzyme formation	151	
	$\beta$ -lactamase	antibacterials	HF, DFT	substrate deacylation reaction	155	
	metallo- $\beta$ -lactamase	antibacterials	DFT/MM	active site features with either zinc or cadmium cation bound	250	
	metallo- $\beta$ -lactamase	antibacterials	DFT(CPMD)	H-bond network determination	160	
	metallo- $\beta$ -lactamase	antibacterials	DFT(CPMD)	protonation state of Asp120	161	
	metallo- $\beta$ -lactamase	antibacterials	DFT/MM-PB	binding of benzylpenicillin	165	
metallo- $\beta$ -lactamase	antibacterials	DFT(CPMD)/MM	hydrolysis of cephotaxime	162		
metallo- $\beta$ -lactamase	antibacterials	DFT/MM	catalytic mechanism and inhibition	164		
metallo- $\beta$ -lactamase	antibacterials	DFT/MM	antibiotic binding to monozinc $\beta$ -lactamase	167		
dihydrofolate reductases	dihydrofolate reductase	anticancers antibacterials antimalarials	PM3/MM	hydride-transfer reaction	251	
	dihydrofolate reductase	anticancers antibacterials antimalarials	EVB/MM	nuclear quantum effect in hydride transfer	183	
	dihydrofolate reductase	anticancers antibacterials antimalarials	AM1/MM	catalytic mechanism	252	
	dihydrofolate reductase	anticancers antibacterials antimalarials	AM1/MM	polarization of the active site by substrate and cofactor	189	
	dihydrofolate reductase	anticancers antibacterials antimalarials	EVB/MM	effect of a single-point mutation	253	
	dihydrofolate reductase	anticancers antibacterials antimalarials	AM1/MM	hydride-transfer reaction	182	
	dihydrofolate reductase	anticancers antibacterials antimalarials	PM3/MM	substrate protonation reaction	254	
	dihydrofolate reductase	anticancers antibacterials antimalarials	EVB/MM	effect of mutation on the hydride transfer reaction	255	
	dihydrofolate reductase	anticancers antibacterials antimalarials	QM/MM	transition state geometrical features	184	
	carbonic anhydrases	human carbonic anhydrase II	diuretics	HF	proton-transfer reaction	256
human carbonic anhydrase II		diuretics	DFT	thermodynamics of Zn <sup>2+</sup> binding	257	
human carbonic anhydrase II		diuretics	DFT/MM	carbon dioxide hydration	258	
human carbonic anhydrase II		diuretics	DFT	proton-transfer reaction	259	
human carbonic anhydrase II		diuretics	PM3/MM DFT/MM	vibrational frequency shift of azide ligand	260	
human carbonic anhydrase II		diuretics	DFT	whole catalytic cycle	261	
human carbonic anhydrase II		diuretics	DFT	COS hydrolysis	262	
human carbonic anhydrase II		diuretics	DFT	comparative study on cadmium and zinc containing enzymes	263	
kinases	cyclin-dependent kinase 2	anticancers	DFT	phosphoryl-transfer reaction	264	

Table 1. Continued

protein family	target biological system	therapeutic area	QM method	studied feature	ref
ribonucleotide reductases	cyclin-dependent kinase 2	anticancers	DFT	features of a series of inhibitors	265
	ribonucleotide reductase I	anticancers antivirals	DFT	inhibition mechanism by ( <i>E</i> )-2'-fluoro-methylene-2'-deoxycytidine-5'-diphosphate	266
	ribonucleotide reductase I	anticancers antivirals	DFT	catalytic role of Glu441	267
	ribonucleotide reductase I	anticancers antivirals	DFT	radical enzymatic mechanism	268
methionine aminopeptidases	ribonucleotide reductase III	anticancers antivirals	DFT	substrate reaction mechanism	269
	methionine	anticancers	DFT	features of the active site containing either cobalt or zinc cation	270
ras	methionine aminopeptidase 1 and 2	anticancers	DFT(CPMD)/MM	inhibition mechanism of epoxides	271
	Cdc42-GAP	anticancers	DFT(CPMD)	GTP hydrolysis	272
	ras-GAP	anticancers	DFT/MM	GTP hydrolysis	273
	ras-GAP	anticancers	HF/MM	GTP hydrolysis	274
	ras-GAP	anticancers	HF/MM	TS and TS analogue geometrical features	275
topoisomerases	topoisomerase I	anticancers	HF, MP2	binding mode of indenoisquinoline	276
	topoisomerase I	anticancers	HF	binding mode of camptothecin (role of $\pi$ - $\pi$ stacking)	277
	topoisomerase I	anticancers	MP2	structure-activity relationships of some camptothecins	278
integrases	HIV-1 integrase	anti-AIDS	DFT	molecular mechanism of phosphodiester bond hydrolysis	279
reverse transcriptases	HIV-1 reverse transcriptase	anti-AIDS	HF/MM	interaction between water and active site residues	280
	HIV-1 reverse transcriptase	anti-AIDS	MP2/MM	drug resistance	281
DNA polymerases	HIV-1 reverse transcriptase	anti-AIDS	HF DFT	binding of efavirenz	282
	DNA polymerase $\beta$	anticancers	HF DFT MP2	active site geometry determination	283
cytochromes	DNA polymerase $\beta$	anticancers	DFT/MD	reaction mechanism	284
	P450cam	drug metabolism	DFT	reaction mechanism from compound 0 to compound I	285
P450	P450 2C, P450 2B, P450 3A	drug metabolism	DFT/MM	electronic and geometric features of compound I	286
	porphyrin model system	drug metabolism	HF DFT	heme parametrization for MM calculations	287
	P450 sterol demethylase	antifungals	DFT	heme parametrization for MM calculations	288
	P450 aromatase	anticancers	DFT	heme parametrization for MM calculations	289
	P450 aromatase	anticancers	DFT	reaction mechanism of the third step of the catalytic cycle	290
	P450cam	drug metabolism	DFT	reaction mechanism of C-H hydroxylation	291
	P450 2B4	drug metabolism	DFT/MM-PB/SA	computations of binding free energy and heme spin state	80
	P450cam	drug metabolism	DFT	camphor hydroxylation	292
	porphyrin model system	drug metabolism	DFT	mechanism of aromatic hydroxylation	293, 294
	P450cam	drug metabolism	DFT, QM/MM	camphor hydroxylation	295
P450cam	drug metabolism	DFT	camphor hydroxylation	292	
P450 3A4	drug metabolism	DFT/MD	metabolism of rapamycin and derivatives	296	

Table 2. Survey (Covering Approximately the Last Four Years) of First Principles QM Applications to Therapeutically Relevant Receptors and Channels

protein family	target biological system	therapeutic area	QM method	studied feature	Ref.
GPCRs	$\delta$ -opioid receptor	analgesics	HF	interaction with a series N-substituted piperidines	195
	ion channels	K <sup>+</sup> channel	DFT	interaction with aminopyridines	225
ion channels	K <sup>+</sup> channel	cardiac	DFT(CPMD)	K <sup>+</sup> permeation	224
	K <sup>+</sup> channel	cardiac	DFT	selectivity filter chemical features	226
nicotinic receptor	nicotinic receptor	anti-Alzheimer	DFT	ligand-receptor interaction	213
	nicotinic receptor	anti-Alzheimer	DFT	ligand-receptor interaction	210
nicotinic receptor	nicotinic receptor	anti-Alzheimer	DFT	binding modeling of multiple species of nicotine and deschloroepibatidine	210

in dealing with modeling aspects of selected targets, and to highlight some representative examples, showing how QM methods have helped to improve the drug discovery process. We believe that computational drug design needs to exploit as many methodologies as possible and to select the ones best suited to tackling each issue. Drug research needs the systematic use of widely different *in silico* tools to facilitate and speed up the discovery process.<sup>2</sup> We hope that chemists willing to apply QM methods in drug design will find in this review the support they need to properly address pharmacologically relevant issues.

## 2. Theoretical Methods

Quantum chemistry offers several methods for calculating electronic properties of biological systems. Among QM methods, one can roughly distinguish *ab initio*, DFT, and

semiempirical approaches. *Ab initio* methods are very accurate but also CPU-demanding, while semiempirical methods are the fastest and, in turn, the least accurate. In the following section, we briefly introduce the main concepts underlying first principles and QM/MM approaches. Interested readers may find a more in-depth description of such methods in several books dealing with quantum mechanics.<sup>25,39-42</sup>

First principles methods can generally be divided into those based on the electronic wave function (*ab initio*) and those focusing on the electron density (DFT). *Ab initio* methods aim at the solution of the Schrödinger equation, which cannot be solved exactly for polyelectronic systems. Therefore, one has to resort to approximations. The simplest one is the Hartree-Fock (HF) approximation, in which the probability of finding an electron is assumed to be independent of the probability of finding other electrons; that is, each electron

feels the average potential of all the other electrons. HF theory accounts for electron–electron interactions only, including the quantum mechanical exchange term but lacking the electron correlation. The correlation energy may then be computed in a variety of ways. For instance, in the Møller–Plesset (MP) many-body perturbation theory,<sup>43</sup> it is treated as a perturbation. Corrections can be made at any order of energy and wave function, and the most commonly applied is the lowest level of correction, MP2, i.e., a second-order Møller–Plesset calculation. Another way to account for the correlation term is to extend the HF approximation to several electron configurations, leading to the so-called multiconfigurational methods. These approaches may reach a very high level of accuracy, but they can also be very CPU-demanding. Indeed, very few applications of QM multiconfigurational computations in drug design have so far appeared in the literature.

A popular way to overcome the neglect of electron correlation effects in HF theory can be found in the DFT framework. The computational effort required by common DFT calculations is similar to that for HF calculations, whereas the accuracy of DFT is much better than that of HF theory and, in some cases, is able to compete with that of multiconfigurational approaches.<sup>44–46</sup> DFT theory dates back to 1964, when Hohenberg and Kohn<sup>47</sup> showed that the ground-state energy of a system of interacting electrons is a unique functional of its electronic density  $\rho(\vec{r})$ . Therefore, the energy depends on only three coordinates (the value of the density at point  $\vec{r}$ ), as opposed to the case of wave function theory (ab initio methods), where the energy depends on the electronic coordinates. Unfortunately, an expression of the energy as a functional of the density is not known. In 1965, Kohn and Sham proposed a way of calculating the density of an imaginary system of  $n$  noninteracting electrons, described by single-particle orbitals  $\varphi_i(\vec{r})$  (the Kohn–Sham (KS) orbitals), which provide the same density (and hence the same energy) of the system under investigation.<sup>48</sup> Within the KS approach, the intricacies of the many-body problem are found in the exchange-correlation term of the functional, for which several different levels of approximation have been proposed. The basic one is the local density approximation (LDA), in which, in each point of the space, the exchange-correlation term is the same as that of a locally uniform electron gas with the same electron density. The LDA severely underestimates the exchange energy and encounters difficulties in describing H-bonding, thus preventing its use in most chemical applications. Great improvement is obtained by making the exchange-correlation term dependent on the density gradient (generalized gradient approximation, GGA). Several gradient-corrected parametrizations are nowadays available, such as, for instance, that of Becke<sup>49</sup> (Becke88), those of Perdew and Wang in 1986<sup>50</sup> (PW86) and in 1991<sup>51</sup> (PW91) for the exchange term, and that of Lee, Yang, and Parr<sup>52</sup> (LYP) for the correlation term. The hybrid B3LYP,<sup>53</sup> which combines 20% of HF and 80% of Becke88<sup>49</sup> exchange functional with the LYP<sup>52</sup> correlation functional, is quite accurate, and its use is rather widespread in quantum chemistry. B3LYP is quite successful in reproducing experimental enthalpies of formation,<sup>54</sup> and it also performs well for other properties, even if reaction barriers need to be confirmed by means of single-point, higher level QM calculations. Nowadays, DFT/B3LYP is widely used to study biological and pharmacological macromolecular systems. DFT was given further expansion when, in 1985,

Car and Parrinello<sup>32</sup> suggested a new method (CPMD) for carrying out MD simulations with forces calculated at the DFT level of theory (for reviews, see refs 55 and 56). This method could be particularly desirable, as it allows one to simulate biological systems at their actual temperatures.

One of the main drawbacks of first principles QM approaches when applied to target-based drug design issues is the neglect of environmental effects such as the protein electrostatic field and the solvent contribution. Actually, QM calculations, either ab initio or DFT-based, are commonly applied to systems of up to 150 atoms, while a model system made by a protein immersed in explicit solvent can reach a typical size of 70,000–100,000 atoms. A possible solution for the modeling of these systems is to partition them into a localized chemically active region (treated with a first principles method) and its environment (treated with an empirical potential). This is the so-called QM/MM approach<sup>33,34</sup> that was first reported in 1976 in a pivotal paper by Warshel and Levitt.<sup>57</sup> In a QM/MM approach, the computational effort is concentrated in the part of the system where it is most needed, whereas the effects of the surroundings are taken into account with a more expedient model:  $H = E_{\text{QM}} + E_{\text{MM}} + E_{\text{QM/MM}}$ . In this equation, the potential energy terms  $E_{\text{MM}}$ ,  $E_{\text{QM/MM}}$ , and  $E_{\text{QM}}$  refer to the classical part, the interaction between QM and MM parts, and the energy of the QM system, respectively. The purely classical part,  $E_{\text{MM}}$ , is described by a standard biomolecular force field. The intricacies of QM/MM methods lie in finding an appropriate treatment for the coupling between QM and MM regions as described by the interaction energy  $E_{\text{QM/MM}}$ . The QM region can be treated at several different levels of theory spanning from semiempirical to ab initio and DFT Hamiltonian. This review will mainly report on first principles QM/MM applications in drug design (most of them at the DFT/MM level of theory). A few select case studies, in which semiempirical QM/MM approaches were employed, will also be reviewed because of the high therapeutical relevance of the investigated biological targets.

### 3. Target-Based Applications of QM Methods

#### 3.1. Enzymes

Enzymes are proteins responsible for the acceleration of biological events by means of a decrease of the activation energy of reaction pathways. In the simple Michaelis–Menten mechanistic scheme,



(where E is the enzyme, S is the substrate, and P is the product), the catalytic constant  $k_{\text{cat}}$  represents the maximum number of substrate molecules converted to products per active site and per unit time. Sometimes, the transformation of ES to E + P involves the formation of intermediates and multiple steps, including the release of the product. In general, the multibarrier reaction path is very different from the noncatalyzed one and by definition has a lower free energy of activation. An in-depth understanding of molecular events at the basis of the catalytic mechanism of enzymes, besides providing a basic explanation of the biological process, might be exploited in practical applications such as the rational design of bioactive compounds. Theoretical methods for simulating enzymatic reactions have evolved rapidly in recent decades. Indeed, electronic quantum effects

have to be taken into account in this field of application to provide a realistic potential energy surface (PES) for the bond rearrangements.<sup>58,59</sup> Typically, in these kinds of calculations, entropic effects are neglected and only a small fraction of minima and TSs of the PES are examined. Moreover, both a quantum treatment of the hydrogen motions, determining tunneling phenomena,<sup>60,61</sup> and relativistic effects should be considered for a fully correct quantum mechanical description of enzymatic reactions. However, these physical aspects are neglected in most theoretical studies carried out on biological systems, which still obtain an in-depth description of the biological event.

Recently, QM-based methods have assumed an increasingly prominent position in the study of therapeutically relevant enzymes,<sup>27</sup> as they may provide insights at the atomistic level about previously unrecognized molecular processes. According to the TS analogues theory,<sup>20,21</sup> a detailed understanding of biocatalysis is expected to provide a framework in which to rationally address enzyme-based drug design, albeit straight applications of either TS structure or electronic features to the enzymatic inhibitor design are so far lacking. In this respect, it is far from certain whether current QM and, in particular, DFT approximations are good enough to determine activation energies and TS features. Concerning DFT-based applications, Car recently stated that “often the DFT description of the transition state is at least qualitatively right”.<sup>62</sup>

Several reviews have appeared concerning computer simulations of enzymatic reactions (see, for instance, refs 63–69). In Table 1, we report a tentative comprehensive survey (covering approximately the last four years) of first principles QM applications to therapeutically relevant enzymes.

Here, we review some applications of QM-based methods to the study of therapeutically relevant enzymes, laying down some perspectives and advancing hypotheses for the exploitation of QM results in rational drug design. The selected case studies show the suitability of QM methods for investigating enzymatic reaction mechanisms as well as for describing electronic and dynamic features of enzyme active sites and for allowing us to present atomistic events that can be properly described by taking into account electronic quantum effects, such as geometries of transition-metal-carrying active sites,<sup>70</sup> proton transfer,<sup>71</sup> and the cation– $\pi$  interaction.<sup>72,73</sup> Moreover, we describe the use of QM methods in studying the quantum hydrogen tunneling phenomenon,<sup>60,61</sup> which is regarded at an increasing pace as a key event at the basis of the catalytic power of enzymes.<sup>74</sup> Finally, we would like to underline that the following section is by no means intended to provide a complete survey of all the computational works in the field of enzymatic reactions. In this respect, some biological systems already have dedicated review articles, such as the cytochrome P450 enzymes,<sup>75–80</sup> which have long been the subject of QM-based computational investigations. Some enzymes of this family are very important targets for therapeutic interventions, while others have a fundamental role in the metabolism of drugs and other xenobiotics and are therefore reported in Table 1. For this topic, the interested reader can refer to reviews such as those of Loew et al.,<sup>75</sup> Segall,<sup>76</sup> Meunier et al.,<sup>77</sup> and Shaik et al.<sup>78</sup> Moreover, Harris very recently reviewed recent progress in the understanding of the structure and mechanism of cytochrome P450s, pointing to the possible future development of reliable QM-based methods for predicting

drug metabolism.<sup>79,80</sup> This would provide computational tools of great usefulness for a drug discovery and development project.

### 3.1.1. Selected Proteases

Proteases are proteolytic enzymes with a central role in living organisms.<sup>81,82</sup> The proteolytic events are essential in the control of cell behavior, survival, and death and, when altered, might be responsible for pathological conditions. Thus, several proteases are currently being investigated in different research fields as targets of pharmacological interest. Since the most widely studied proteases in computational drug design are the aspartic proteases, particularly the HIV-1 aspartic protease, and the serine proteases, some applications of QM-based calculations on these targets are presented here. Furthermore, QM studies on cysteine proteases (e.g., caspases) are also reported, due to the emerging role of these enzymes as potential and innovative pharmacological targets for anticancer and anti-Alzheimer therapies.

**HIV-1 Aspartic Protease.** In the field of anti-AIDS therapies, HIV-1 protease represents the main therapeutic target on which medicinal chemistry research has been focused in recent years. The most intriguing feature of this enzyme, which bears a dimeric structure, is the presence of a catalytic dyad composed of two aspartic acids (one per monomer: Asp25 and Asp25<sup>1</sup>) (Figure 1), which activate a water molecule to give a nucleophilic attack to the substrate. The HIV-1 protease reaction mechanism and protein dynamics have been extensively studied by one of the present authors.<sup>83–86</sup> A recent review reports on the main achievements of this work.<sup>87</sup> A fundamental observation concerns the catalytic dyad, which is supposed to be protonated on one of the two aspartic acids. Recently, Sirois et al.<sup>88</sup> calculated, by means of QM/MM computations, the relative energies between two different protonation sites of Asp25 and Asp25<sup>1</sup> of the catalytic dyad for several HIV-1 protease–inhibitor complexes. First, the protonation site preference was evaluated by increasing the size of the model system. This demonstrated that the protonation site preference was always in favor of the inner oxygen of the aspartic acid with respect to the outer one; however, the energy difference was strongly dependent on the model system size. With the smallest model system (15 atoms), the energy difference was as wide as 23.5 kcal/mol, decreasing to 5.3 kcal/mol with one of the largest systems (67 atoms) investigated. Interestingly, in the apo-enzyme, which bears a different crystallographic symmetry when compared to an enzyme–inhibitor complex, the energy difference decreased to 3.4 kcal/mol. Increasing the size of the model system and introducing hydrophobic residues around the catalytic center (105 atoms) did not affect the energy difference. This is in good accord with previous observations by Piana et al.,<sup>85</sup> who also demonstrated that the backbone surrounding the active site is very rigid, thus demonstrating the suitability of a relatively small model system in the gas phase for studying the features of the HIV-1 protease active pocket. Furthermore, Sirois et al. also demonstrated that the interaction energy within the catalytic site is predominantly due to hydrogen bonds and electrostatic interactions, pointing to a network of H-bonds among the active site residues, the drug, the tetracoordinated water, and the enzyme flaps. Finally, the authors hypothesized the presence of a key water molecule in the active site of some protease–inhibitor complexes. This last finding is significant for the design of new protease inhibitors, since a water

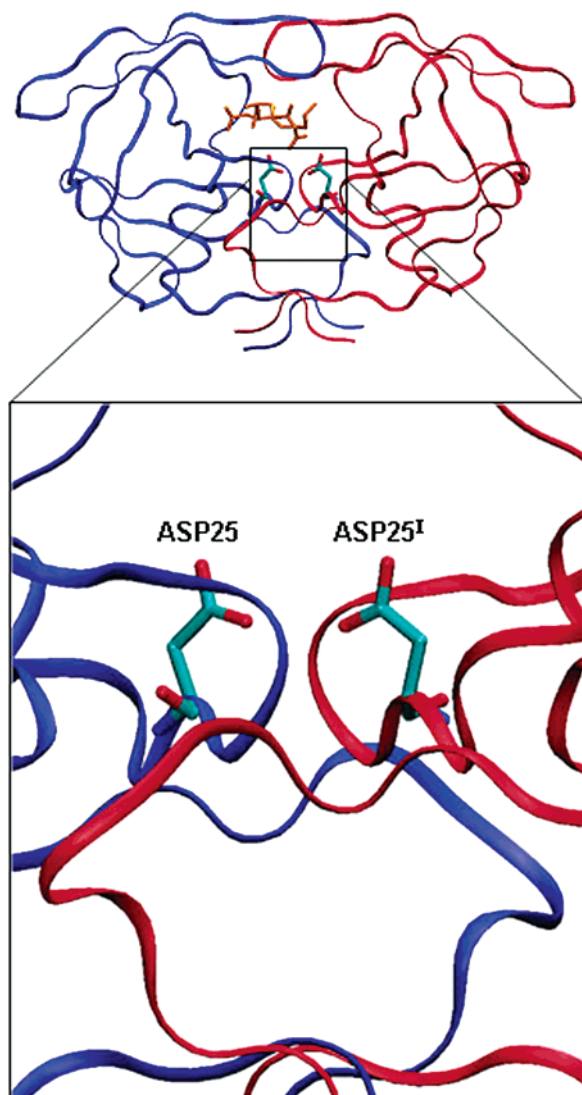


**Figure 1.** 3D structure of HIV-1 protease complexed with a tripeptide inhibitor (orange) (PDB code 1A30). The enzyme is a homodimer (the chains are colored in red and blue) related by a  $C_2$  symmetry axis. The peptide cleavage site shown at higher magnification is located at the subunit interface. Only the aspartate residues of the catalytic dyad (Asp25 and Asp25') are explicitly displayed.

molecule appropriately replaced by an ad hoc moiety can provide a gain in both enthalpy and entropy to the interaction free energy, as shown for the protease inhibitor XK-263 active at the picomolar level.<sup>89–91</sup>

An invaluable contribution to the present computational methods is represented by the possibility of improving the accuracy of docking (and virtual screening) scoring functions by means of QM calculations. Recently, Andreoni and co-workers reported on the possibility of enhancing the accuracy of a force field-scoring procedure through QM-based calculations. The authors validated the new methodologies by predicting the activity of a set of HIV-1 protease inhibitors.<sup>92</sup> A similar study was also carried out by Raha and Merz. These authors used quantum mechanics at a semiempirical level of theory to improve a scoring function for docking simulations. Testing the resulting scoring function on several protein–ligand complexes (among which were 26 HIV-1 protease–ligand complexes), the authors could calculate the electrostatic interactions and solvation free energy expected upon complexation.<sup>93</sup> Again, it was shown that QM could

ameliorate docking scoring functions, and it is likely that, in the future, the routine use of QM-based scoring functions will greatly improve the accuracy of the computational ligand design step in the drug discovery process.<sup>93</sup>

Two further interesting papers dealing with first principles calculations and drug design reported on investigations concerning inhibitor–HIV-1 protease interactions. In the first paper, written by Zhang and Zhang, the authors reported a full QM study of the interaction between HIV-1 protease and six FDA-approved drugs (i.e., saquinavir, indinavir, ritonavir, amprenavir, and lopinavir). The study was conducted at both HF/3-21G and B3LYP/6-31G(d) levels of theory, following the molecular fractionation with conjugate caps (MFCC) approach, which was developed recently by the authors.<sup>94,95</sup> This method provides an easy means of deriving interaction energies between individual protease residues and drugs. First, a detailed study was carried out to determine the interaction energy of the HIV-1–lopinavir complex. Starting from the enzyme–inhibitor cocrystal, the authors could lay down some important general rules for the interaction of this drug with its biological counterpart. In particular, the lopinavir OH group could form a strong H-bond interaction with Asp25 of chain A of the enzyme. In addition, a second H-bond interaction was observed between the drug and Asp29. Then, the other five FDA-approved drugs were investigated using the MFCC approach; namely, the drugs were divided into four building blocks connected by the central component containing the pivotal hydroxyl group. By investigating in depth the contribution of each building block to the interaction energy, it would be possible to design new inhibitors by properly combining and modifying such structural blocks. In the second paper, the interaction energy between TMC114, a new generation inhibitor, and HIV-1 protease was computed at the HF and DFT levels of theory.<sup>96</sup> The results were also compared with the interaction energies estimated for the nelfinavir– and amprenavir–HIV-1 protease complexes. It emerged that TMC114, structurally related to amprenavir and bearing a novel bis-tetrahydrofuranyl group, could form, with the backbone hydrogen of Asp29, a further H-bond interaction, which was probably responsible for TMC114's greater inhibition potency when compared to the other two drugs.

**Serine Proteases.** The proteases bearing a nucleophilic serine residue at the active site are commonly called serine proteases and represent almost one-third of all known proteases. Serine proteases are probably the most thoroughly investigated enzyme system. The mechanism of action of these enzymes involves a so-called catalytic triad composed of an aspartic acid, a histidine, and the catalytic serine residue (using chymotrypsin numbering, Asp102, His57, and Ser195; see Figure 2).

Recently, however, serine proteases bearing novel catalytic triads and dyads have been discovered.<sup>97</sup> It is widely accepted that serine proteases work through a common general mechanism, which accounts for an acylation (Figure 3A) and a deacylation (Figure 3B) step. During the acylation step, a nucleophilic attack of the hydroxyl group of the catalytic serine on the carbonyl carbon of the substrate leads to the formation of the acyl-enzyme adduct, which is hydrolyzed by a water molecule during the deacylation reaction. The commonly accepted mechanism for either acylation or deacylation accounts for a two-step reaction with two transition states and a tetrahedral intermediate stabilized by

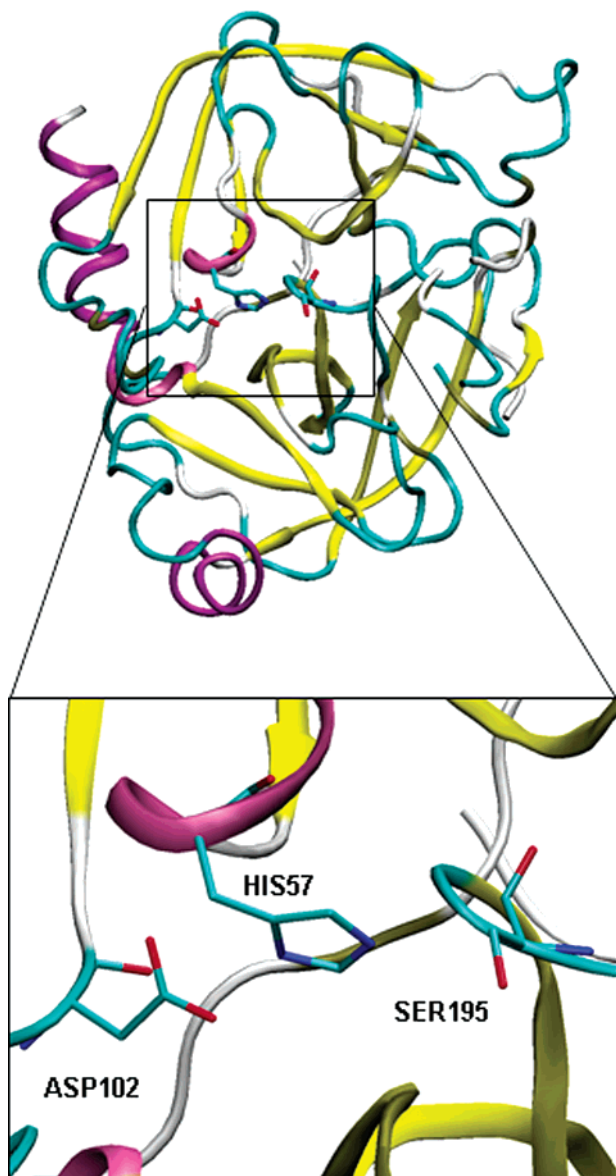


**Figure 2.** 3D structure of the serine protease  $\gamma$ -chymotrypsin at 1.80 Å resolution (PDB code 1K2I). The coloring method highlights the secondary structure motifs, following the default color code of the VMD software.<sup>297</sup> The catalytic triad (Asp102, His57, and Ser195) is shown at higher magnification, and the residues are displayed in sticks.

means of H-bond and electrostatic interactions with active site residues forming the so-called “oxyanion hole”.

Recently, both acylation and deacylation reactions catalyzed by serine proteases have been investigated by means of QM/MM calculations.<sup>98,99</sup> A QM/MM approach was needed, as environmental effects turned out to be fundamental to stabilizing the tetrahedral intermediate. Interestingly, studying the same mechanism in the gas phase, Topf and Richards demonstrated that the reaction proceeded through a single step, and the stable tetrahedral intermediate was no longer isolated.<sup>99</sup> Moreover, both studies<sup>98,99</sup> employed sampling methods (i.e., free energy perturbation and umbrella sampling), which also accurately estimate entropic effects. In such a way, the activation barriers were estimated from the free energy rather than from the PES. For both acylation and deacylation reactions, the rate-limiting event was the formation of the tetrahedral intermediate and the calculated reaction barriers turned out to be in good agree-

ment with the experimental ones. In conclusion, these studies show that QM/MM methods combined with either free energy perturbation or umbrella sampling allow one to account for environmental effects, to accurately estimate the entropy, and, finally, to calculate a realistic free energy profile associated with a certain biological reaction.

While both studies<sup>98,99</sup> reported the results of the separated steps (acylation and deacylation) of serine proteases' catalytic cycle, Nemukhin et al., in early 2004, reported a QM/MM study of the entire enzymatic cycle.<sup>100</sup> The interested reader may find in the Introduction section of this paper<sup>100</sup> a detailed description of the literature (including papers from before 2001) concerning QM studies of serine proteases. Furthermore, the authors reported the results of their QM/MM calculations carried out in the framework of the effective potential theory.<sup>101</sup> Several QM/MM selections were taken into account by the authors, as different partitioning schemes could provide different outputs. Actually, with the first model investigated (40 atoms at QM level), the authors succeeded in describing the complete reaction path for the investigated serine protease. However, they failed to accurately estimate the activation barrier of the rate-limiting step. With the second model system employed, in which both the QM (56 atoms) and MM parts were enlarged, the authors reasonably estimated the energetic of the acylation step, which is considered to be the rate-limiting step of the entire catalytic cycle.

The QM/MM results reported in these studies<sup>98–100</sup> might be of paramount importance for the design of TS analogue inhibitors of pharmacologically relevant serine proteases. Indeed, recent papers report on syntheses of compounds that are able to inhibit serine proteases and that bear geometrical and physicochemical features of the enzymatic TS.<sup>102–105</sup> Clearly, the design of similar inhibitors might be properly addressed by exploiting the results of reaction mechanism studies. To this end, we propose that the docking of TS analogues at the serine protease active site in the TS configuration, followed by the estimation of the binding free energy, may greatly enhance both the understanding of the SARs of new inhibitors and the design of chemical modifications to provide more potent bioactive compounds. Moreover, QM studies on the reaction mechanism of serine proteases might also shed light on the main reaction steps of cholinesterases (also called serine hydrolases) such as the acetylcholinesterase (AChE) enzyme, which holds a relevant place in contemporary medicinal chemistry research,<sup>106</sup> and butyrylcholinesterase (BChE), which is gaining renewed interest as a putative therapeutic target.<sup>107,108</sup>

The most attractive therapeutic target among the serine protease-type enzymes is the hydrolase AChE.<sup>109</sup> Due to its involvement in the central neurotransmission, AChE inhibition has been exploited at the therapeutic level in the field of Alzheimer's disease.<sup>110</sup> Since the pioneering work of Höltje and Kier, who were able to hypothesize, by means of semiempirical QM calculations, a cation- $\pi$  interaction between the cationic head of ACh and an aromatic residue in the enzyme binding site,<sup>111</sup> a large number of computational studies have appeared in the literature, even though most of them address the dynamic behavior of the AChE protein.<sup>112</sup> However, the mechanism of action has also been widely investigated, with AChE being one of the fastest known enzymes.<sup>109</sup> This enzyme catalyzes the hydrolysis of the neurotransmitter ACh with a second-order reaction-rate constant close to the diffusion-controlled limit.<sup>109</sup> Recently,



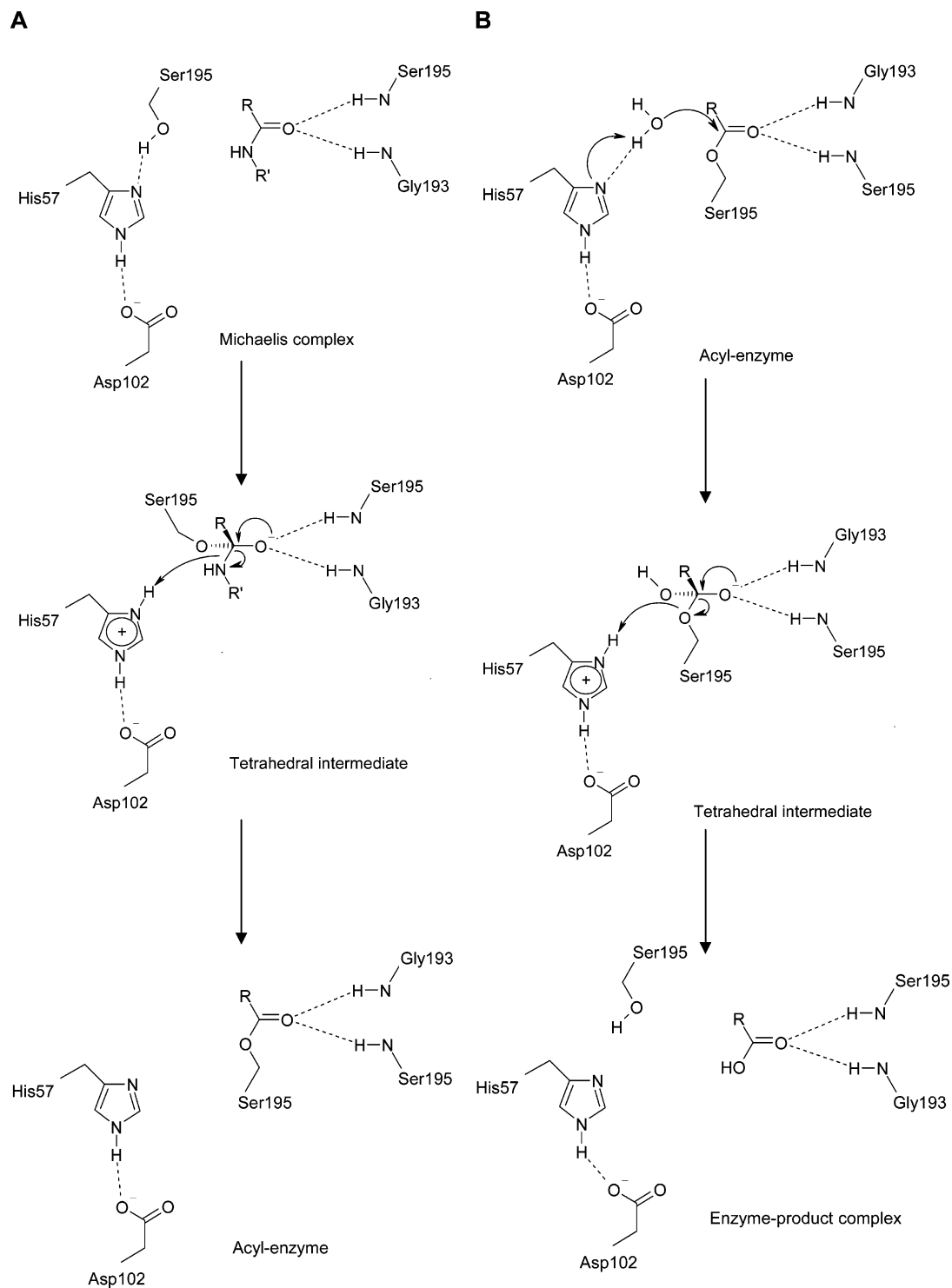


**Figure 3.** Serine protease catalytic mechanism (the numbering of  $\gamma$ -chymotrypsin is used). (A) Acylation step. Ser195, activated by means of an H-bond network with His57 and Asp102 (the catalytic triad), carries out nucleophilic attack on the carbonyl carbon of the substrate. The tetrahedral intermediate internally rearranges to lead to the acyl-enzyme adduct. (B) A water molecule regenerates the free enzyme by hydrolyzing the acyl-enzyme. This reaction proceeds via a tetrahedral intermediate species.

the initial step of the acylation process catalyzed by AChE was investigated by means of QM/MM calculations, which estimated the potential energy barrier at the MP2/6-31G\* level of theory.<sup>113,114</sup> The calculations carried out by McCammon and co-workers revealed that, as expected, the acylation step occurred through nucleophilic attack of Ser203 (according to the human AChE numbering) at the carbonyl carbon of the substrate. A proton transfer from Ser203 to His447 increased the nucleophilic character of Ser203, which could perform the attack leading to the tetrahedral intermedi-

ate. The estimated energy barrier for the first step was in very good agreement with the experimentally determined one (10.5 vs 12 kcal/mol). Glu334 stabilized the reaction TS by means of electrostatic interaction, thus seemingly disproving a charge-relay mechanism involving a proton transfer from His447. Interestingly, in a smaller model system investigated in this study, Glu334 was treated molecular-mechanically; however, it captured most of the stabilization energy of the reaction TS. This further demonstrated the involvement of Glu334 in electrostatic interaction with His447, thus disprov-

ing a proton-transfer reaction between the residues. Finally, the study by McCammon's group showed that the peptidic NH groups of Gly121, Gly122, and Ala204 formed a three-pronged oxyanion hole, with only the hydrogen atoms of Gly121 and Gly122 directly involved in H-bonds with the carbonyl oxygen of ACh. Ala204 NH was shown to play a crucial role as the reaction proceeded. The distance between hydrogen and the oxygen became shorter, and the third hydrogen bond was formed with both the TS and the tetrahedral intermediate. The results of McCammon and co-workers clearly support very similar mechanisms between serine proteases and hydrolases. Recently, Wang et al. investigated, at the B3LYP/6-311G(d,p) level of theory, the binding of fasciculin-2 (*fas-2*) at the external surface of *Torpedo californica* AChE.<sup>115</sup> In addition, single-point MP2 calculations were performed on the DFT-optimized geometries. The interaction energies were accurately estimated through the Kitaura–Morokuma scheme.<sup>116</sup> First, the authors computed the interaction energy between loop 1 of *fas-2* and the enzyme to be  $-99.4$  kcal/mol. This value could well account for the very good experimentally observed affinity constant (0.0023 nM) of *fas-2* toward AChE. Second, the authors pointed to Thr8 of *fas-2* as the pivotal residue for anchoring the inhibitor at the external surface of the enzyme. Finally, through the Kitaura–Morokuma decomposition analysis, they could suggest that the electrostatic term provided the main contribution to the total interaction energy. From a drug design perspective, the present results may be very interesting. Actually, noncatalytic functions of AChE are seldom taken into consideration, even though they might be of some therapeutic relevance, as demonstrated by the AChE peripheral anionic site involvement in the Alzheimer's  $\beta$ -amyloid protein precipitation.<sup>117</sup>

Very recently, BChE, another cholinesterase enzyme, has been the subject of QM investigation. BChE is the primary cocaine-metabolizing enzyme present in human blood, and it provides inactive cocaine through a hydrolysis reaction. Aimed at designing a BChE mutant bearing higher efficiency toward cocaine when compared to the wild-type enzyme, Gao and co-workers first studied the BChE-catalyzed reaction mechanism of cocaine hydrolysis using QM/MM calculations.<sup>118</sup> The reaction involves the nucleophilic attack of the catalytic serine to the ester group of cocaine. The energy barriers of this reaction were evaluated at the MP2/6-31G\* level of theory, treating the MM part of the system with the Amber force field.<sup>119</sup> The environmental effects were of crucial importance for a correct estimate of the energy barriers, which were in good agreement with available experimental data. The authors conclude that the first reaction step is very close to the rate-limiting one (the third step) and that it was so sensitive to the protein environment that such a step could actually be the rate-limiting one for cocaine hydrolysis catalyzed by a BChE mutant. With this in mind, in a following study, they proposed a designed mutant of the BChE enzyme endowed with an increased activity toward cocaine.<sup>120</sup> To this end, they carried out MD simulations on the binary TS–BChE complex, and based on the outcomes of these simulations, they finally designed an enzyme mutant. The BChE mutant showed a significantly improved catalytic efficiency toward cocaine when compared to the wild type, thereby demonstrating that TS simulation is a promising approach for rational enzyme redesign and drug discovery.<sup>120</sup> Designing either a ligand or a protein with high affinity

toward the counterpart in the TS configuration may provide tight binding protein–ligand complexes.

Finally, when reviewing QM studies on serine proteases, a comment is required on the so-called low barrier hydrogen bond (LBHB) and its role in enzymatic reactions. An LBHB is characterized by a shorter distance between the heteroatoms involved ( $<2.65$  Å) compared to that for a regular H-bond (Figure 4A) and bears a more covalent character

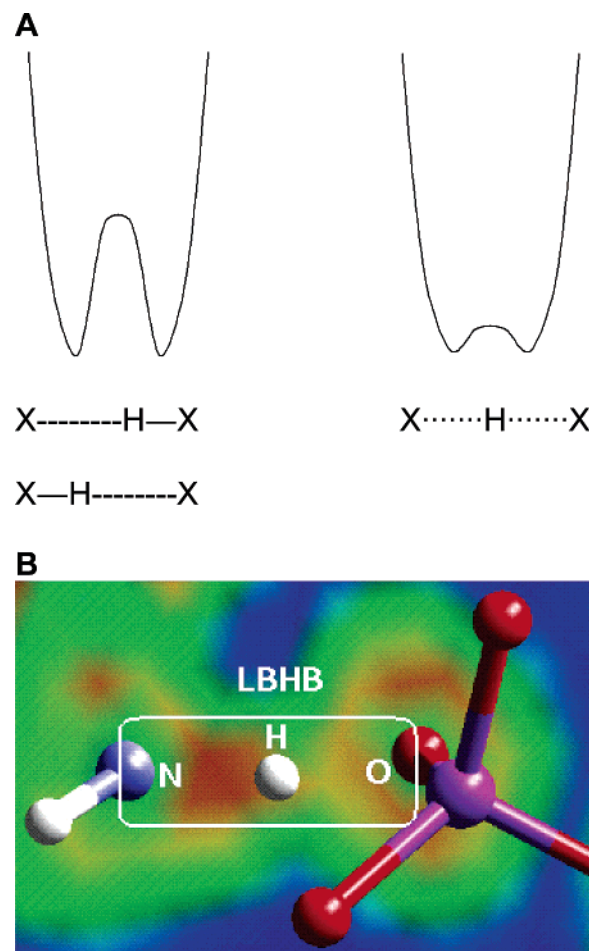


**Figure 4.** (A) Energy diagrams for hydrogen bonds between groups of equal  $pK_a$ . When the distance between the two heteroatoms ( $X = N, O$ ) involved in an H-bond is higher than 2.8 Å, the interaction is quite weak (left diagram), whereas when such a distance is less than 2.55 Å, a low barrier hydrogen bond (LBHB, right diagram) is present: the hydrogen is diffusely distributed with an average position in the center. (B) Representation of a low-barrier hydrogen bond (LBHB) during enzymatic catalysis. The picture refers to the LBHB between Lys16 and the GTP during the GTP hydrolysis catalyzed by the G-protein Cdc42. Figure adapted from ref 272. The red and blue areas indicate strong and weak electron localization, respectively.

accompanied by a more dispersed charge distribution (Figure 4B). Moreover, an LBHB requires the absence of an aqueous environment and a very small difference between the  $pK_a$  values of the heteroatoms involved (close to zero). LBHBs could, in principle, be very important for stabilizing the enzymatic reaction TS.<sup>71,121–123</sup>

In computational chemistry, LBHBs can be detected only by means of accurate QM-based methods, as they require a full treatment of quantum electronic effects to properly describe polarization and charge-transfer processes. In serine proteases, the LBHB hypothesis states that, during the catalysis, the transformation of the Asp102–His57 H-bond

in an LBHB may stabilize the reaction TS and lower the activation free energy. This hypothesis is mainly (but not only) based on NMR measurements, in which the shared proton shows a large low-field chemical shift, a low fractionation factor, and a positive value for the deuterium isotope effect.<sup>124–130</sup> On the contrary, the QM-based calculations reviewed here<sup>98,99,131,132</sup> disprove such an interaction, since the distance is longer than that of an LBHB and the shared hydrogen is mainly localized on the His57 nitrogen. However, for this reaction mechanism, it might be concluded that a strong H-bond interaction exists between Asp102<sup>-</sup> and His57<sup>+</sup> during the reaction path and that such an interaction is fundamental for the catalytic process: seemingly, defining H-bonds as LBHBs might sometimes be a matter of interpretation.<sup>133</sup>

**Cysteine Proteases.** Cysteine proteases are an enzyme family involved in several biological processes. Imbalances in the normal expression and function of human cysteine proteases, or involvement of parasitic or viral cysteine proteases are associated with a variety of pathological conditions.<sup>134</sup> In drug design, there is growing interest in this protein family since inhibition of these enzymes might represent an important strategy for the treatment of a variety of human diseases. For instance, programmed cell death, commonly defined as apoptosis, is a normal biological process regulated by the caspases protein family (“c” is intended to reflect a cysteine proteases mechanism, whereas “aspase” refers to the ability to cleave the substrate after an aspartic acid).<sup>135</sup> Some diseases, such as cancer or neurodegeneration, are characterized by an anomalous functioning of programmed cell death processes, and for this reason, caspases have emerged as possible targets for pharmaceutical intervention.

Analogously to serine proteases, cysteine proteases bear, in the active site, a sort of catalytic triad (Figure 5), which is always composed of a histidine that accepts a proton from the cysteine (the second amino acid of the triad) during the nucleophilic attack carried out by it. The third component of the triad is a residue accepting an H-bond from the histidine. This may be a conserved asparagine, such as in the case of papain-like enzymes,<sup>136</sup> or a residue, whose backbone acts as H-bond acceptor. The lack of a negatively charged residue present in the serine protease active site might be due to the fact that the essential proton transfer between the catalytic cysteine (more acid than a serine) and the general base histidine might involve a lower barrier with respect to that of the serine–histidine system. It has been demonstrated that, in the serine protease enzyme, the lack of Asp102 in the Asp102Asn mutant reduces the proton-transfer efficiency, with the catalysis still being possible, although with a higher energy barrier.<sup>131</sup> As with serine proteases, the reaction mechanism is thought to occur in two steps, the acylation and the deacylation.

Recently, CPMD-based QM/MM calculations have been carried out to study the second reaction step (the deacylation, i.e., the hydrolysis of the acyl-enzyme adduct) of the enzymatic reaction catalyzed by caspase-3.<sup>137</sup> The activation free energy was calculated by means of the thermodynamic integration technique, thus allowing an accurate estimation of the TS barrier. This study shows that the attack of the catalytic water molecule to the acyl-enzyme goes through a previously unrecognized gem-diol intermediate species and involves an activation free energy of ca. 19 kcal/mol. Interestingly, this result is in good agreement with available

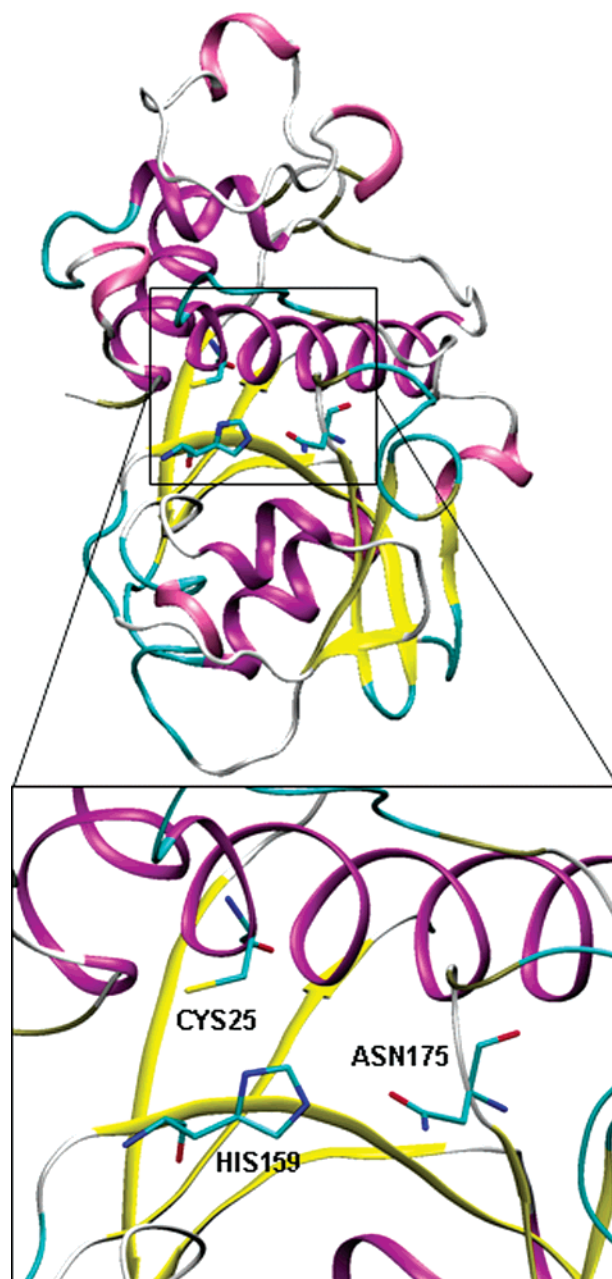


**Figure 5.** 3D structure of the cysteine protease papain at 2.10 Å resolution (PDB code 1POP). The coloring method highlights the secondary structure motifs, following the default color code of the VMD software.<sup>297</sup> The catalytic triad (Cys25, His159, and Asn175) is shown at higher magnification, and the residues are displayed in sticks.

experimental data for this reaction and is very similar to the same reaction step in the serine protease enzyme.<sup>99</sup> From a medicinal chemical view, the most interesting finding concerns the identification of the gem-diol intermediate. First, the structural and electronic features of such an intermediate might be exploited to design caspase inhibitors able to tightly bind to the enzyme active site as TS analogues. Second, since this intermediate is a peculiar feature of the caspase mechanism, the rational design based on its electronic and structural properties is expected to provide selective inhibitors. A comment is required on the accuracy of the methodology used here and is summarized in the following points: (i) the BLYP approximation for the exchange-correlation functional, which is known to underestimate the TS energies;<sup>86</sup> (ii) the choice of the initial configuration used

for the QM/MM simulations, in which the reactants were already in a favorable position; (iii) a simplified one-dimensional reaction coordinate that limited the calculation of the energy profile to one constrained MD trajectory. Concerning the latter point, it is known that, for a more accurate estimate of the activation energy, several paths should be considered;<sup>138,139</sup> such a protocol is, computationally, very demanding.

Concerning the design of cysteine protease inhibitors, Helten et al.<sup>140</sup> recently studied, at the DFT level, the ring-opening reactions of three-membered heterocycles that can be used as irreversible peptidomimetic inhibitors of this enzyme family.<sup>136</sup> In particular, the authors estimated the energies of ring-opening reactions for different three-membered heterocycles, studying the nucleophilic attack to the cycles carried out by the sulfur atom of the catalytic cysteine. Besides providing a consistent explanation for the experimental results for thermodynamic constants and the regioselectivity of ring-opening reactions, the study might also be useful for predicting different potencies of cysteine protease inhibitors that carry an epoxide, an aziridine, and a thiirane three-membered heterocycle. In our opinion, the study of Helten et al.<sup>140</sup> may be considered an interesting example of QM computations providing the basis for the rational design of molecules potentially useful in therapy.

### 3.1.2. Penicillin-Binding Proteins (PBPs) and $\beta$ -Lactamases

Penicillin-binding proteins (PBPs) and  $\beta$ -lactamases are enzymes able to interact with  $\beta$ -lactams, like, e.g., penicillins and cephalosporins. These enzymes share a similar folding, and a great problem with these protein families concerns their capability to rapidly mutate, thus making bacteria resistant to the antibiotic action.<sup>141</sup> PBPs carry out the final steps of bacterial cell wall assembly.<sup>142</sup> Their target role is to catalyze the formation of the cross-linked peptidoglycan of the bacterial cell wall.  $\beta$ -Lactams act as pseudosubstrate and covalently bind to a serine residue (acylation reaction) within the active site, thus inhibiting PBPs enzymatic activity. On the contrary,  $\beta$ -lactamases are enzymes elaborated by bacteria. They represent an effective strategy for conferring bacterial resistance as they rapidly destroy up to  $10^3$  molecules of penicillin per second. These enzymes are responsible for most resistance against  $\beta$ -lactams, thus seriously compromising the efficacy of antibacterial chemotherapy.<sup>143–145</sup>  $\beta$ -Lactamases are classified into four classes, with those of class B being metallo- $\beta$ -lactamases, whereas classes A, C, and D (serine- $\beta$ -lactamases) and PBPs are commonly called active site serine enzymes.<sup>146</sup>

An in-depth understanding of the molecular mechanism of both PBPs and serine- $\beta$ -lactamases might be very important for identifying the amino acids likely to undergo mutations and, therefore, for designing new ligands capable of binding to mutated active sites. Despite the structural and ligand-binding similarities, an interesting difference between PBPs and serine- $\beta$ -lactamases concerns their catalytic efficiency. The overall catalysis is composed of two steps (Figure 6): (i) the acylation (Figure 6A), in which the catalytic serine gives nucleophilic attack to the  $\beta$ -lactam ring, affording the acyl-enzyme adduct; (ii) the deacylation (Figure 6B), in which the acyl-enzyme is hydrolyzed by a catalytic water molecule, leading to the free enzyme and to inactive antibiotics, i.e., a molecule bearing an opened  $\beta$ -lactam ring. Actually, while serine- $\beta$ -lactamases rapidly catalyze hy-

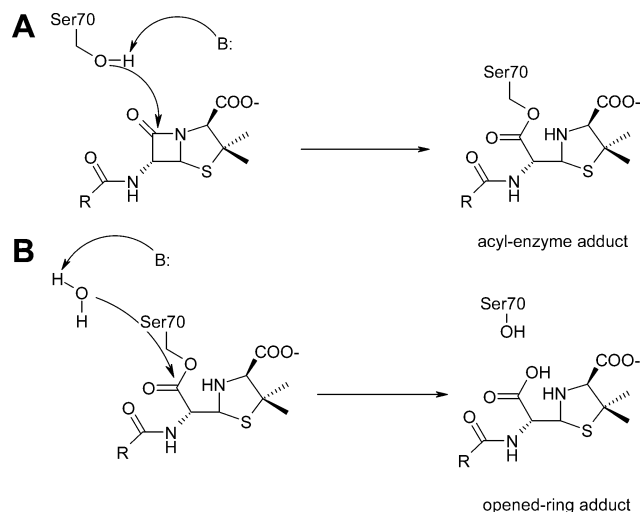


**Figure 6.** Mechanism of the  $\beta$ -lactam ring hydrolysis. (A) Acylation step: Ser70 carries out nucleophilic attack on the  $\beta$ -lactam ring of penicillins. (B) A water molecule regenerates the free enzyme by hydrolyzing the acyl-enzyme. Both reactions are supposed to proceed via a tetrahedral intermediate species.

drolisis of the acyl-enzyme intermediate, PBPs are very poor catalysts of this reaction and are effectively trapped in the acyl-enzyme intermediate and thus inactivated. This means that the deacylation step is very efficient in serine- $\beta$ -lactamases, whereas such a reaction is practically absent in PBPs. From a drug design perspective, gaining insights into such a reaction-rate difference and, more generally, into PBP and serine- $\beta$ -lactamase enzymatic mechanisms may facilitate the development of new antibiotics not susceptible to  $\beta$ -lactamase hydrolysis but still able to efficiently bind even mutated PBPs.

The acylation step of the catalytic mechanism of PBPs was recently studied by means of several different computational approaches ranging from MD simulations to the Poisson–Boltzmann approach to pure QM calculations, which provided details about the catalytic mechanism.<sup>147</sup> This study points to a fundamental role for the relatively conserved Glu166 (according to the class A  $\beta$ -lactamases numbering), which turned out to be protonated even at pH 8 and which played a direct chemical role both in the formation of the tetrahedral intermediate and during the subsequent acylation. However, by also taking into account solvation effects, the pathway that utilizes Lys73 as a general base appeared to be the energetically favored one, thus pointing to the possibility of multiple reaction mechanisms. To shed further light on this enzymatic reaction step, Höltje, Mulholland, and co-workers recently studied, by means of QM/MM calculations, the full acylation reaction step.<sup>150</sup> This study was carried out in the QM/MM framework using the semiempirical AM1-CHARM22 method,<sup>148</sup> and the estimated potential energy surfaces were corrected using DFT-based methods at the B3LYP/6-31+(d) level of theory. The computations were performed keeping the physiological protonation state of Lys73 (namely, +1), and the authors unequivocally demonstrated that Glu166 acts as the general base deprotonating a conserved water molecule, which in turn is able to take out a proton from the catalytic Ser70.<sup>149,150</sup> This key observation was found to be in good agreement with experiments. The energy barriers of the overall PES were also very similar to those measured experimentally, when high-level DFT corrections were introduced. At the DFT level, the TS of the overall process was identified to

be the proton transfer from Ser70 to the conserved water molecule. Therefore, designing  $\beta$ -lactams able to increase the energy of this event, by means of a local electric field, would probably provide antibiotics that were more stable to the  $\beta$ -lactamase action. Among other findings, Hermann et al. also identified a possible oxyanion hole similar to that usually described for serine protease enzymes. In particular, two NH amide groups of Ser70 and Ala237 were found to stabilize the negative charge of the substrate carbonyl group of 15.2 kcal/mol in the tetrahedral intermediate species. Most of the conclusions drawn from this work were recently confirmed by Meroueh et al., who carried out a QM/MM study of the same reaction using penicillanic acid as a substrate.<sup>151</sup> The study was carried out at the high QM level MP2, while the MM part was treated with the Amber force field.<sup>119</sup> However, two main differences should be pointed out: (i) Meroueh et al. showed that a mechanism involving Lys73 as a general base in the reaction is fully viable, while this mechanism was disproved by Hermann et al.;<sup>149,150</sup> (ii) Meroueh et al. demonstrated that the catalysis intermediates are less stable than the Michaelis complex, in contrast to what was reported by Hermann et al. The slight differences in these results might be related to the QM/MM methods and model systems investigated by the two groups.

As previously mentioned, from the therapeutic application point of view, the deacylation process represents a key step on which to focus, as this is almost absent in PBPs, whereas it is very fast in  $\beta$ -lactamase enzymes. This step was recently investigated by Friesner and co-workers, who studied the reaction between the antibiotic cephalotin and both PBPs and serine- $\beta$ -lactamases aimed at identifying at an atomic level the main factors responsible for different reaction rates.<sup>152</sup> In particular, the authors investigated the step of the intermediate formation, which is thought to be the one that limits the deacylation reaction rate. The study was performed using a QM/MM approach as implemented in the Jaguar suite.<sup>153</sup> The QM part was treated at the DFT/B3LYP level of theory while the MM part was studied by means of the OPLS-AA force field.<sup>154</sup> First, the authors showed that, as expected, the activation energy was much higher in an aqueous environment than in the enzyme and that, in the  $\beta$ -lactamase enzymatic complex, such a barrier was 14.3 kcal/mol, in perfect agreement with the experimental value. Besides the fortuitous character of such an agreement between computations and experiments, this study further shows that a DFT/MM approach is capable of properly estimating bond forming/breaking processes and also is able to account for environmental electrostatic effects affecting the energetics of an enzymatic reaction. With PBP, the activation energy was 40 kcal/mol, about 13 kcal/mol higher than the experimental one (27 kcal/mol). However, such a difference clearly explains the much higher catalytic efficiency of serine- $\beta$ -lactamases toward the deacylation process when compared to PBPs. From a medicinal chemical perspective, this may assist with the drug design of new and more effective antibiotics. Indeed, following the procedure presented by these authors, one may design a new antibiotic and compute the activation energy for the deacylation step in  $\beta$ -lactamases and PBPs. All chemical modifications will be addressed in such a way as to increase the barrier height of the  $\beta$ -lactamase-catalyzed reaction (while checking that new compounds will not be hydrolyzed by PBPs), eventually providing irreversible inhibitors able to permanently block the  $\beta$ -lactamase activity. Finally, it is worth mentioning a

more recent study carried out by Hata et al., in which the whole deacylation step was studied by means of QM calculations (the system was previously equilibrated by means of classical molecular dynamics simulations), shedding further light on this key step of the serine- $\beta$ -lactamase reaction.<sup>155</sup>

**Zn(II)- $\beta$ -lactamase.** Among metallo- $\beta$ -lactamases, much attention has been given to the study of Zn(II)- $\beta$ -lactamase, one of the new generation of enzymes developed by antibiotic-resistant bacteria.<sup>156</sup> These enzymes very efficiently catalyze the hydrolysis of the four-membered  $\beta$ -lactam ring with consequent loss of effectiveness against the target microorganisms. As with other classes of  $\beta$ -lactamases, metallo- $\beta$ -lactamases are able to rapidly mutate at the catalytic site, increasing the efficiency of the hydrolytic action.<sup>157</sup> A common feature of this protein family is the presence of one (Figure 7A) or two (Figure 7B) Zn(II) ions in the active site, which activate the catalytic water molecule for the nucleophilic attack at the  $\beta$ -lactam ring.

Both the mononuclear and binuclear forms of the enzyme have been recently and independently studied using QM-based methods by Merz's and Carloni's groups.<sup>158–162</sup> Although both carried out calculations within the DFT framework, Merz's group made use of the Gaussian98 suite of programs,<sup>163</sup> whereas Carloni's group performed MD simulations with the CPMD method.<sup>32</sup> The sizes of the investigated model systems were also slightly different, with the one studied by Carloni's group being a bit wider, as the second-shell ligands were also included. In most respects, these independent studies led to similar results. However, it is worth discussing some slight differences concerning the protonation state of conserved residues coordinating the Zn(II) cation.

Concerning the mononuclear form of the enzyme (Figure 7A), Merz and co-workers proposed a mechanism in which the  $\beta$ -lactam ring is hydrolyzed by attack of the zinc-bound hydroxide ion with a concomitant proton transfer from the doubly protonated His210 to the leaving amino group.<sup>158</sup> In contrast, for this form of the enzyme, Carloni and co-workers suggested that a positively charged His210 would strongly compete with the salt bridge between Arg91 and Asp90, thus making the histidine residue not optimally oriented to assist the catalysis.<sup>160</sup> According to this study, neutral His210 would more accurately describe the structural determinants of the mononuclear form of Zn(II)- $\beta$ -lactamase. Moreover, a novel mechanism for the hydrolysis was recently proposed on the basis of CPMD-based QM/MM calculations.<sup>162</sup> The interesting feature pointed out by the study was the expansion of the zinc coordination sphere by a water molecule during the first step of the reaction. Such a feature may be very important for the design of new inhibitors, which are expected to bear a moiety mimicking the presence of this further coordinating water molecule. The displacement of a water molecule from a protein active site may result in an increase of the ligand–target interaction free energy as a consequence of both entropic and enthalpic gain.

Concerning the binuclear form of the enzyme (Figure 7B), Merz and co-workers discovered that a protonated aspartic acid (Asp120) in the Zn(II)-coordinating shell provides a more fluctuating behavior of the active site through the breaking and/or forming of the Zn1–OH–Zn2 bridge. The authors assumed that such a flexibility could be favorable for substrate binding and catalysis, and thus, they hypothesized that this residue might be neutral in the native form

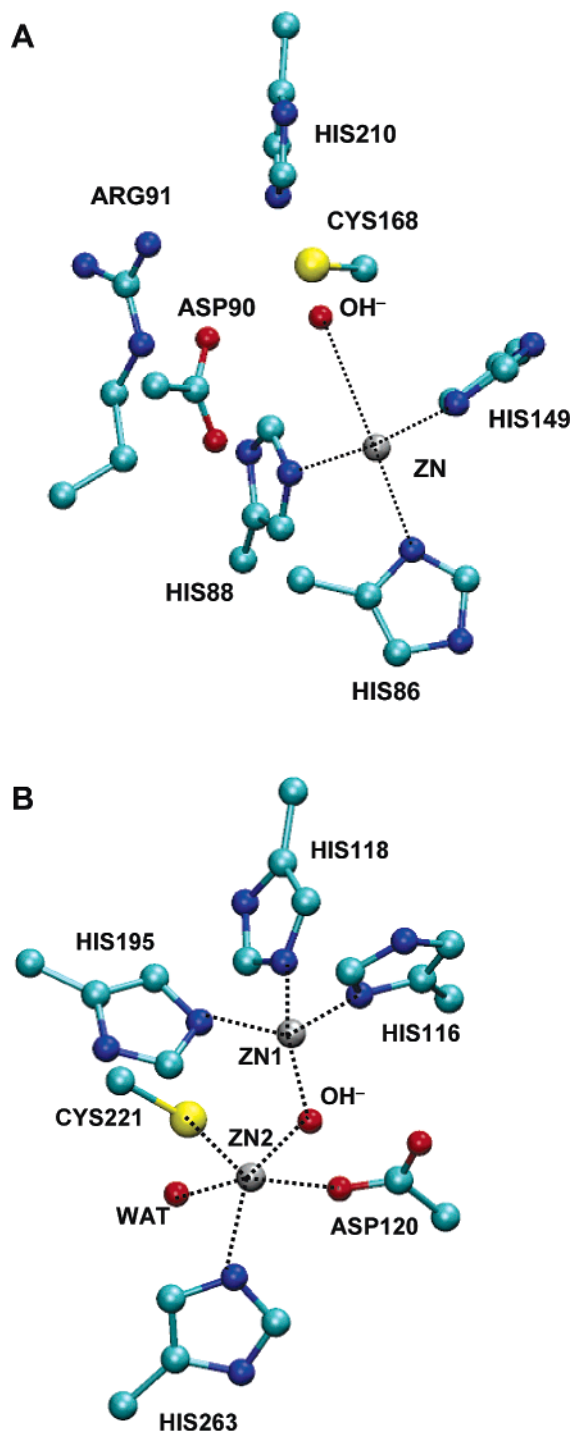


**Figure 7.** (A) Ball and stick representation of the active site of the mononuclear Zn(II)- $\beta$ -lactamase from *Bacillus cereus* (PDB code 1BMC; for the sake of clarity, only the active site side chains are shown). The zinc cation is tetrahedrally coordinated with His86, His88, His149, and a hydroxide anion. (B) Ball and stick representation of the active site of the binuclear Zn(II)- $\beta$ -lactamase from *Bacteroides fragilis* (PDB code 1ZNB; for the sake of clarity, only the active site side chains are shown). One zinc cation (ZN1) is tetrahedrally coordinated with His116, His118, His195, and a hydroxide anion, while the other one is pentacoordinated in a bipyramidal configuration with Asp120, Cys221, His263, a hydroxide anion, and a neutral water molecule.

of the enzyme.<sup>159</sup> In contrast, the DFT calculations carried out by Carloni and co-workers supported a mechanism that relied on a deprotonated negatively charged aspartic acid. Structural analyses showed that the protonation of the aspartic

acid disrupted the bonding features with the Zn2, which were well-preserved with the deprotonated form.<sup>161</sup>

As shown, the conclusions of these studies are not in complete agreement and further calculations might be needed to definitively resolve the outstanding issues.

In the field of Zn(II)- $\beta$ -lactamase inhibitors, the bridge between QM and computational drug design seems imminent. In this respect, it is worth mentioning a further paper by Merz and co-workers<sup>164</sup> and a paper by Ryde and co-workers.<sup>165</sup> In the first study, the authors, besides investigating the reaction mechanism of binuclear Zn(II)- $\beta$ -lactamase, carried out docking simulations followed by DFT-based computations of the thiazolidinecarboxylic acid (TCA) nanomolar inhibitor bound at the enzyme active site.<sup>164</sup> While docking simulations were performed with the AutoDock program,<sup>166</sup> the DFT computations were done with the Jaguar suite.<sup>153</sup> In this way, Merz and co-workers could investigate structural and energetic features of the binding of the inhibitor at the binuclear Zn(II)- $\beta$ -lactamase active site. They showed that the initial binding of TCA at the enzyme active site could involve some interactions very similar to those established by the dinuclear Zn(II)- $\beta$ -lactamase substrate, with the sulfur of the inhibitor side chain being tightly bound to the zinc ions by means of a strong electrostatic interaction. In the paper by Ryde and co-workers, the authors investigated the binding of benzylpenicillin to mononuclear forms of this protein family by means of combined docking and QM/MM simulations.<sup>165</sup> First, they docked benzylpenicillin into the Zn(II)- $\beta$ -lactamase active site by means of the AutoDock program,<sup>166</sup> and then they carried out MD simulations at the MM level and electrostatic calculations employing the Poisson–Boltzmann equation. Finally, the authors minimized the geometry of the benzylpenicillin/Zn(II)- $\beta$ -lactamase binary complex with a QM/MM approach, treating the binding pocket at the DFT/B3LYP level of theory and the surroundings with the Amber force field.<sup>119</sup> As expected, the MM and MD structures were quite different from the QM/MM ones, particularly for the interactions between ligands and Zn<sup>2+</sup>. Actually, interactions of ligand-coordinating transition metals such as the Zn<sup>2+</sup> cation are hard to describe reliably by means of classical MM force fields. In this respect, the paper points out the importance of using QM/MM refinement calculations in the docking of ligands to metal-carrying proteins. Since a wide number of pharmacological targets bear a metal ion in the active site, the need to apply accurate QM calculations to such biological systems is clear.

Recently, Xu et al. also studied, at the QM/MM level, the interactions occurring at the binary complex between the antibiotic biapenem and a mononuclear Zn(II)- $\beta$ -lactamase.<sup>167</sup> Starting from the X-ray crystallographic structure of the enzyme complexed with a product of biapenem hydrolysis,<sup>168</sup> Xu et al. built a proper docking model resembling the Michaelis enzyme–inhibitor complex. Then, the authors investigated the dynamics of the active site of both the apoenzyme and the binary complex between Zn(II)- $\beta$ -lactamase and biapenem. The study was carried out using an alternative QM/MM approach based on self-consistent charge density functional tight binding, also taking advantage of the recent parametrization of the zinc cation for simulating biological systems.<sup>169</sup> This method is based on DFT-computed charge variation, and the interested reader may refer to the original paper by Elstner et al.<sup>169</sup> In the study by Xu et al., to provide an independent check of this alternative

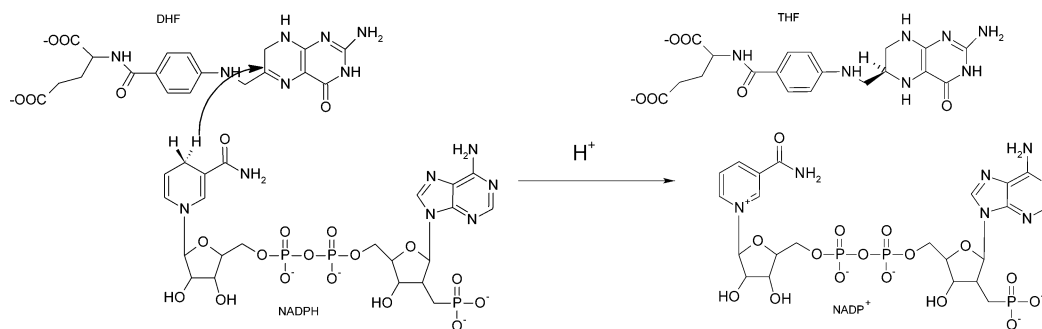


**Figure 8.** Schematic representation of the hydride transfer between NADPH and DHF. The reaction is supposed to be enhanced by hydrogen tunneling effects, giving NADP<sup>+</sup> and THF.

QM/MM method, DFT calculations were also carried out, at the B3LYP/6-31+G(d) level of theory, on both the biapenem and a truncated active site model system.<sup>167</sup> The results obtained with the different methods were in fairly good agreement.

### 3.1.3. Dihydrofolate Reductase

Dihydrofolate reductase (DHFR) has long been a pharmacological target investigated in depth by means of several different computational approaches, ranging from classical MD simulations to more recent DFT-based QM/MM calculations. Recently, Schnell, Dyson, and Wright have reviewed the structure, dynamics, and catalytic function of DHFR.<sup>170</sup> DHFR catalyzes the reduction of the 7,8-dihydrofolate (DHF) to 5,6,7,8-tetrahydrofolate (THF) through the oxidation of the coenzyme nicotinamide adenine dinucleotide phosphate (NADPH).<sup>171</sup> In the drug discovery field, this enzyme holds a prominent position because of its relevance as a target for anticancer,<sup>172</sup> antibacterial,<sup>173</sup> and antimalarial<sup>174</sup> agents. The fundamental role of DHFR is to maintain the intracellular level of THF, which is an important cofactor in the biosynthesis of purines, thymidylate, and several amino acids. The overall reaction catalyzed by DHFR involves the addition of a proton and a hydride ion to DHF, leading to THF. Since the 1980s,<sup>175–177</sup> the reaction mechanism of DHFR has been investigated in depth by means of computational approaches. The main aspects of the catalysis have been explored, showing that the reaction involves several steps and chemical processes. An interesting aspect concerns the only ionizable residue of the active site, Asp27, which was hypothesized to be responsible for a proton-transfer pathway. This scenario was recently supported by Gready and co-workers, who addressed the issue of the protonation state of the conserved acidic residue (Asp or Glu) during both reactions, the reduction of folate to DHF, and the reduction of DHF to THF.<sup>178,179</sup> These studies were conducted at the DFT/B3LYP level of theory, confirming the results by means of calculations with the MP2 method. The authors support a mechanism for both folate and DHF reductions, in which the carboxylate group of the acidic residue is first protonated and then a direct protonation occurs at N8 of the folate and N5 of DHF. Eventually, the protonation of DHF makes the key hydride-transfer (Figure 8) reaction step easier.

This result was further confirmed by a work in which the PES of the reaction was modeled by means of a mixed QM/MM approach. Summarizing these studies, it may be concluded that the reduction of DHF occurs through an initial proton transfer, followed by the hydride transfer, thus disproving the alternative mechanism in which the hydride transfer should occur first.<sup>180,181</sup> In particular, these calcula-

tions show that the free energy barrier is 30 kcal/mol higher for deprotonated than for protonated DHF. In a recent paper by Garcia-Viloca et al.,<sup>182</sup> another finding worth mentioning was the important role of quantum mechanical vibrational effects (i.e., quantum hydrogen tunneling) that lowered the energy barrier of the hydride-transfer reaction by 3 kcal/mol. This was in very good agreement with previous QM/MM dynamics simulations carried out by Hammes-Schiffer and co-workers, who suggested a significant multidimensional quantum tunneling contribution to the hydride-transfer rate.<sup>183</sup> In further and more recent studies, Truhlar, Gao, and co-workers studied, by means of QM/MM calculations, the geometrical features of the TS of the hydride-transfer reaction in DHFR.<sup>184</sup> In this work, they used the hybridization state of the carbon atom involved in the hydride transfer as a complementary reaction coordinate. In the authors' opinion, the use of this coordinate reaction has some advantages relative to the sole use of bond distances and charge development as progress measures in hydride-transfer reactions.<sup>185</sup> Applying this approach, the authors showed that the donor carbon at the hydride-transfer TS resembled the reactant state more than the product state, in disagreement with the hypothesized secondary kinetic isotope effects. In our opinion, these computations<sup>184,186</sup> allowed a deeper interpretation of experimental results from kinetic isotope effect investigations, demonstrating a good complement between theory and experiment toward an enhanced understanding of complex quantum biochemical processes.

Quantum mechanical tunneling is a phenomenon in which a light particle transfers through a reaction barrier thanks to its wavelike properties, which are associated with the dual nature of the matter. In the classical model of chemical reactions involving particles surmounting a thermodynamic barrier, the reacting species must have enough thermal energy to reach the TS. Conversely, if a barrier is sufficiently narrow compared with the wavelength of a particle, there is a finite probability that the particle can find itself on either side of the barrier without having to surmount it; that is, the particle can be transferred by quantum mechanical tunneling. Since the wavelength of a particle is inversely proportional to its mass, quantum mechanical tunneling has thus far only been inferred for reactions involving very light particles. This is well-established for electrons, whose wavelength is 18 Å, transferred solely by QM tunneling, whereas it is controversial for the hydrogen atom whose wavelength is 0.5 Å. However, based on experimental observations that a certain behavior cannot be explained without invoking hydrogen tunneling, several studies identified QM transfer of hydrogen in enzymatic systems.<sup>60,61</sup> In particular, enzymes that catalyze different reactions via different mechanisms and an ac-

accompanying charge transfer appear to utilize tunneling, thus adding new features to the conventional view of enzyme catalyses. Indeed, much experimental and theoretical data suggest that enzymes have evolved to impose critically controlled active site structures and dynamics to enhance tunneling. Recently, Hammes-Schiffer reviewed MM and QM methods to study nuclear quantum effects in biological systems.<sup>187</sup> In this article, the interested reader may find a survey of the main computational approaches to the study of quantum tunneling effects. Again, QM/MM approaches are among the most promising methods for studying this quantum phenomenon in biological systems, where environmental effects may play a pivotal role. However, it is outside the scope of the present review to discuss in depth the quantum effects in chemical and biological processes, and the interested reader may refer to more specialized literature.<sup>58,188</sup>

Recently, Truhlar and co-workers also investigated, by means of combined QM/MM simulations, the effects of the protein electric field (environmental effects) of DHFR on the electronic polarization of the 5-protonated DHF substrate at various stages of the catalyzed hydride transfer.<sup>189</sup> Actually, to enhance an understanding of enzyme–substrate interactions, as well as the molecular mechanism of the catalysis, it is of great interest to investigate the effects of the protein electric field on both the electronic structure and the molecular polarization of the substrate, the active site residues, and the possible cofactor at various stages of a reaction. In this paper, the authors describe, by means of QM/MM and MD simulations, average polarization effects at the reactant, the TS, and the product alongside the reaction of hydride transfer. MD simulations were carried out on both the reactant and the product complexes. The TS species was also simulated by means of MD, while restraining the complex with a harmonic potential. The most interesting finding of this paper concerns the large polarization energy identified. Although this constituted only 4% of the interaction energy, it is large in absolute magnitude, because the combined substrate–cofactor system is a highly charged species. This study concludes that it is essential to consider electron polarization effects in order to understand and model enzyme–substrate interactions and catalysis. From a drug discovery perspective, the evaluation of polarization effects could be very important for properly addressing the rational design of bioactive compounds. As mentioned above, TS analogue inhibitors might be the tightest binders to an enzyme. Therefore, evaluating the polarization effects for the amino acid active site and fitting partial point charges on these residues at the TS configuration may provide the best framework for identifying ligands by means of conventional docking and virtual screening simulations. The output hits will be the compounds that best fit the protein active site in the TS rather than in the Michaelis configuration.

### 3.2. Receptors and Channels

In the field of computational drug design, applications of QM-based methods to the study of both receptor features and receptor–ligand interactions are fairly limited when compared to the applications of QM-based methods to the study of enzymes (see Tables 1 and 2).

This can be explained both by the small number of solved crystal structures of receptors (which are needed as a reliable starting point for any QM calculation) and by the lack, in most cases, of specific reaction mechanisms involving bond

forming/breaking to be investigated. Therefore, the main applications of QM-based methods to the study of receptors of pharmacological relevance concern in-depth investigation of certain interactions and phenomena that are only just captured by force field-based calculations. For instance, some QM-based studies were devoted to determining the contribution of the cation– $\pi$  interaction, which can be partially accounted for by means of MM methods but which can be quantitatively investigated only by explicitly taking into account polarization effects, charge transfer, and electron clouds. The cation– $\pi$  interaction represents a noncovalent force that accounts for the strong attraction exerted by a  $\pi$  cloud of an aromatic ring on a positively charged moiety, such as simple and small cations (e.g.,  $\text{Li}^+$ ) or complex organic structures (for instance, the ammonium head of acetylcholine).<sup>72,73,111</sup> Concerning organic amines, it is worth remembering that ammonium cations make for a weaker interaction when compared to protonated amines.<sup>190</sup> The cation– $\pi$  interaction holds a prominent position among the noncovalent interactions operating in biological systems. What may still be surprising is that aromatic moieties can compete with an aqueous environment in binding cations by means of a cation– $\pi$  interaction.<sup>72</sup> As early as 1981, Sunner et al. showed that, in the gas phase, the  $\text{K}^+$ –water and  $\text{K}^+$ –benzene attraction energies were 18 and 19 kcal/mol, respectively.<sup>191</sup> The origin of the cation– $\pi$  interaction is mainly due to the attraction between the negatively charged  $\pi$  cloud of the aromatic ring and the positively charged cation. This implies that many physicochemical aspects have to be considered to properly describe such an interaction. Basically, the cation– $\pi$  interaction can be considered as an electrostatic effect that involves the quadrupole moment of the aromatic ring. In this respect, an ion–quadrupole interaction can be described by means of a classical force field with all hydrogen atoms explicitly treated (the so-called all-atom model). Although this treatment can be qualitatively correct, it has been clearly demonstrated that additional terms, such as induced dipole, polarizability, dispersion forces, and charge transfer, have to be included to quantitatively describe the interaction.<sup>192</sup> Importantly, the ion–quadrupole term is a very specific distance-dependent interaction, as it is expected to drop off as  $1/r^3$ . In contrast, the cation– $\pi$  interaction exhibits a  $1/r^n$  dependence with  $n < 2$ , thus resembling a Coulombic interaction ( $1/r$ ) rather than an ion–quadrupole interaction.<sup>72</sup> However, some of the present authors have recently demonstrated that a properly parametrized ion–quadrupole interaction, mimicking a cation–indole interaction (Figure 9), is accurate enough to estimate the free energy profile of the tetramethylammonium penetration of the human AChE enzyme<sup>193</sup> by means of metadynamics simulations.<sup>194</sup>

In the following paragraphs, we review some recent studies on receptors that treated the cation– $\pi$  interaction at the QM level. As above, we report on works regarding receptors and channels of pharmacological relevance.

#### 3.2.1. Receptors

The nature and the strength of the cation– $\pi$  interaction have been investigated recently by Mo et al., who studied a series of N-substituted piperidines in complex with a model system representing the  $\delta$ -opioid receptor.<sup>195</sup> This receptor belongs to the superfamily of G-protein coupled receptors, whose computational and modeling studies received renewed interest<sup>196,197</sup> after the X-ray determination of the structure



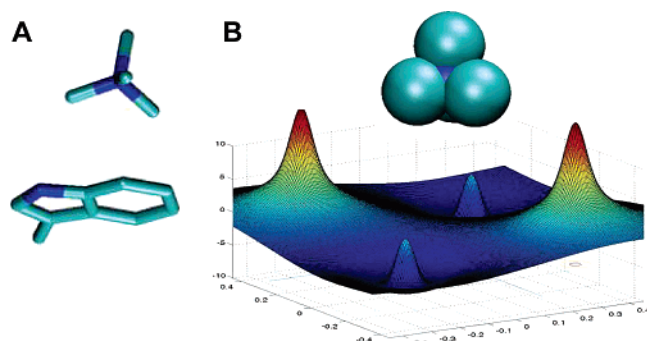


**Figure 9.** Cation– $\pi$  interaction between (A) tetramethylammonium (TMA) and the indole ring, along with (B) a qualitative representation of the potential landscape generated by an electric quadrupole. Arbitrary units are reported in the 3D plot. Picture conceived by Dr. W. Rocchia at the Scuola Normale Superiore di Pisa (Italy).

of the rhodopsin protein.<sup>198</sup> For a long time, it was supposed that the  $\delta$ -opioid receptor interacted with protonated biogenic amines through a salt bridge with an ionized aspartic or glutamic acid. A recent study revealed that this assumption is no longer true, as a single mutation of the Asp128 in the TMIII did not affect the binding of positively charged amines.<sup>199</sup> Therefore, a possible cation– $\pi$  interaction was hypothesized. In particular, attention was devoted to the nearby Tyr129, as a single mutation of this residue impairs the binding of biogenic amines to the  $\delta$ -opioid receptor.<sup>200</sup> In the study by Mo et al., ab initio calculations at the HF/6-31G\* level of theory were performed on model systems that mimic the binding environment around Tyr129. The authors also investigated the single contribution to the free energy of interaction between differently substituted aromatic centers and a positively charged piperidine by means of an energy decomposition analysis. This was carried out using a purposely developed block-localized wave function method,<sup>201</sup> implemented into the GAMESS software package.<sup>202</sup> The authors clearly demonstrated that the cation– $\pi$  interaction is significant for most of the investigated systems with energies ranging from 6 to 12 kcal/mol. Also, in this case, the cation– $\pi$  interaction could be energetically competitive with a classical salt bridge, in agreement with previous findings in an aqueous environment.<sup>203</sup> The energy decomposition into electrostatic, polarization, and charge-transfer terms provided further interesting findings. The traditional view that the electrostatic energy is the dominant one was also confirmed for the  $\delta$ -opioid receptor system. However, this interaction alone accounts for 40–58% of the total energy, and it is thus fundamental to consider other contributions too. In particular, the polarization energy turned out to be about 30% of the total energy, whereas the contribution of the charge transfer from the  $\pi$  system to the cation was as much as 16–25%. Interestingly, Mo et al. also noticed that electrostatic and polarization energies are almost linearly correlated to the total interaction energy, whereas the charge-transfer contribution appeared to be constant.

The present results raise the question of how the simple electrostatic model employed in the classical force fields can accurately represent the cation– $\pi$  interaction, if polarization and charge-transfer contributions are so relevant. The energy decomposition carried out by Mo et al. clearly reveals that there is a linear correlation between electrostatic and polarization energies and that these two terms account for most of the interaction energy of a cation– $\pi$  interaction. On one hand, it may be argued that classical force fields can be adequately used to investigate biomolecular systems, as

suggested earlier.<sup>72</sup> However, on the other hand, it must be concluded that specific contributions should be investigated in greater detail to provide a quantitative estimate of the interactions in which polarization and charge transfer take place to a relevant degree. In computational drug design, a way to address this issue might be to carry out docking and MD simulations employing empirical potentials to pose ligands (agonists and antagonists) and to study their dynamic behavior within a receptor binding pocket, and to eventually refine the results by means of QM or, better, QM/MM calculations, when quantum electronic effects need to be accounted for (such as, for instance, when cation– $\pi$  interactions are involved).

### 3.2.2. Ion Channels

**Nicotinic ACh Receptor.** The nicotinic ACh (nACh) receptor, the prototype of the ligand-gated ion channels, has long been investigated as a target of therapeutic interest.<sup>204</sup> Nowadays, in particular, the neuronal nicotinic receptors are investigated as targets for a variety of impairments at the neuronal level.<sup>205</sup> A great number of aromatic amino acids are present in the ACh binding site, as demonstrated by the recent crystal structure of the ACh-binding protein (AChBP) of the snail *Lymnaea stagnalis* alone<sup>206</sup> and in complex with nicotine, carbamylcholine, and *N*-2-hydroxyethylpiperazine-*N*-9-(2-ethansulfonic acid) (HEPES).<sup>207</sup> The crystal structures as well as recent homology and docking models clearly show the involvement of a cation– $\pi$  interaction between the ACh neurotransmitter and the AChBP binding pocket.<sup>208–210</sup> Further experimental evidence shows, in contrast, that nicotine is greatly stabilized within the AChBP binding pocket by means of an H-bond interaction with the carbonyl backbone of Trp $\alpha$ 149.<sup>207</sup> Therefore, it seems that “cholinergic” ligands might bind at the receptor in a different fashion from that for “nicotinic” ones. This issue has recently been investigated by Dougherty and co-workers, who carried out a combined experimental and QM-based computational study to identify the binding differences between nicotinic and cholinergic agonists.<sup>211</sup> It was shown that, while ACh interacts by means of a pivotal cation– $\pi$  interaction with the indole ring of Trp $\alpha$ 149,<sup>212</sup> nicotine and epibatidine experience an H-bond interaction with the backbone carbonyl of the same residue. Moreover, epibatidine also shows a cation– $\pi$  interaction comparable to that observed for the ACh neurotransmitter, which is able to explain the 100-fold potency of epibatidine relative to nicotine.<sup>211</sup>

In addition, Morreale et al. recently carried out QM calculations to describe the interaction energies of the binding of ACh, nicotine, and epibatidine at the agonist neuronal nicotinic receptor site.<sup>213</sup> Using an average model for the agonists, as obtained by previous MM and MD simulations,<sup>214</sup> the interactions at the binding site were accurately estimated by means of single point calculations at the DFT/B3LYP level of theory. Again, this study points to a relevant contribution of the cation– $\pi$  interaction between the cationic head of ACh and the indole ring of the tryptophan residue located at the ligand binding pocket.

A further interesting study was carried out in 2005 by Zhan and co-workers.<sup>210</sup> The authors used homology modeling, docking, and first-principles calculations to study the binding of nicotine and deschloroepibatidine at the neuronal  $\alpha$ 2 $\beta$ 4 nACh receptor binding pocket.

As shown in Figure 10, nicotine and deschloroepibatidine can exist in six and four different molecular species able to

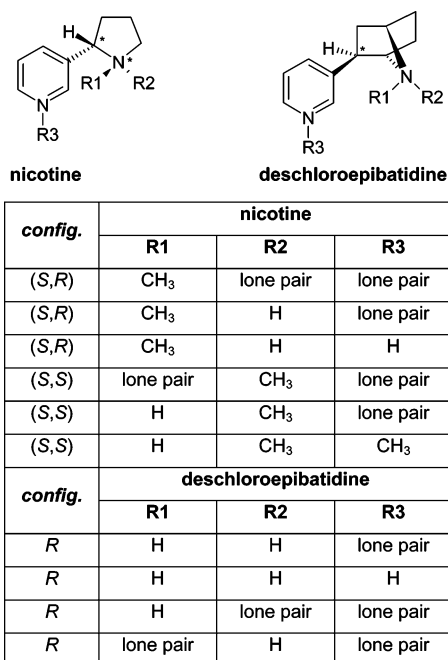


**Figure 10.** Structures of the six and four molecular species of *S*-nicotine and *R*-deschloroepibatidine, respectively, used in the study of ref 210.

interact with the biological counterpart. Besides confirming that H-bonding and cation- $\pi$  interactions play a central role in the binding of the ligands, they were able to demonstrate that all molecular species of nicotine and deschloroepibatidine (Figure 10) can quickly reach a thermodynamic equilibrium both in solution and at the  $\alpha 2\beta 4$  nACh receptor binding pocket. Notably, the pH played a fundamental role in determining the protonation states of the two ligands. Once the thermodynamic equilibrium concentration was assessed, the authors focused on the determination of the microscopic binding free energies of all different molecular species of nicotine and deschloroepibatidine. They found a good correlation between the calculated microscopic binding free energies and the “phenomenological” (i.e., experimental) affinities of nicotine and deschloroepibatidine for the  $\alpha 2\beta 4$  nACh receptor. This approach, named by the author “from-microscopic-to-phenomenological”, was in our opinion very well-suited for the issue under investigation, and it may represent a new accurate approach for the design of ligands (potential drugs) targeting the  $\alpha 2\beta 4$  nACh receptor.

Computational studies on nicotinic receptors were actually boosted by the determination of the crystallographic structure of the AChBP.<sup>206,207</sup> However, it should be highlighted that AChBP is a small soluble protein with less than 25% of sequence identity with the neuronal nACh receptor. Therefore, much attention should be given when laying down hypotheses or conclusions based on homology-built models using the AChBP template.<sup>215</sup> The cross-check of homology models with the available experimental literature is usually a good rule, which becomes a strict requirement in the modeling of nicotinic receptors. However, the previously mentioned studies clearly point to a pivotal role for the cation- $\pi$  interaction in the binding of ligands at the nACh receptor binding pocket. As shown, this interaction can be described qualitatively by means of classical MM simulations. However, if a quantitative agreement is required, the cation- $\pi$  interaction has to be investigated in greater depth by means of QM-based computations.

**Voltage-Gated Ion Channels.** Voltage-gated ion channels are at the basis of a variety of physiological processes because of their regulation of the fluxes of specific ions across the cell membrane.<sup>216</sup> Voltage-gated K<sup>+</sup> channels are involved in an increasing number of channelopathies, and therefore, both the general mechanisms of ion channels and their potential role as pharmacological targets are receiving increased interest in the life sciences.<sup>217</sup> In recent years, computational studies on K<sup>+</sup> channels have appeared in the literature at an increasing pace,<sup>216</sup> thanks to the seminal work carried out by MacKinnon’s group, who solved the X-ray structures of several of these membrane proteins.<sup>218–223</sup>

QM-based calculations at the DFT level of theory have recently been applied to the study of structural and electronic aspects of K<sup>+</sup> permeation through the KcsA channel,<sup>224</sup> as well as to the determination of the receptor sites responsible for the channel blocking by protonated aminopyridines.<sup>225</sup> The latter is a theoretical work carried out by Munoz-Caro and Nino and performed at the B3LYP/6-311G\*\* level of theory both in vacuo and in water solution. The authors investigated two hypotheses of interaction advanced on the basis of crystallographic analysis. In particular, the cationic head of the aminopyridines can interact either through a salt bridge with the anionic moiety of a glutamic acid residue or by means of a cation- $\pi$  interaction with an aromatic residue of the channel. The results clearly disprove the formation of a salt bridge between the glutamic acid and the cationic head, since such an interaction would involve a variation of free energy both in vacuo and in solution incompatible with the in vitro activity. In contrast, a combination of cation- $\pi$  interaction and H-bonding provides a far better explanation for the experimental data. Again, the fundamental role of cation- $\pi$  interaction in biological systems is highlighted.

More recently, Ban et al. studied the physicochemical features of the KcsA channel entrance and release of K<sup>+</sup> and Na<sup>+</sup> ions using DFT-based computations at the B3LYP level of theory.<sup>226</sup> Earlier, Guidoni and Carloni showed, by means of DFT calculations, that K<sup>+</sup>-induced polarization effects played an important role in the cation permeation.<sup>224</sup> In the study of Ban et al., the authors were able to demonstrate that the selectivity between K<sup>+</sup> and Na<sup>+</sup> begins with the entrance of the cation into the selectivity filter. This process is energetically more favored by 2.7 kcal/mol for K<sup>+</sup> when compared to Na<sup>+</sup>.

Studying the interaction of ligands with voltage-gated ion channels is an issue of great medicinal chemical interest, opening a path to computational studies of the interaction of drugs with channels of pharmacological or toxicological interest. For instance, in recent years, the critical role that the K<sup>+</sup> channels might play in drug-induced cardiac toxicity has emerged clearly.<sup>227</sup> The need for accurate tools able to predict the likelihood of newly designed compounds to interact with this antitarget protein is now widely recognized, and accurate computational methods might be effectively exploited to this end.<sup>228–230</sup>

#### 4. Conclusions and Outlook

More than other chemical disciplines, computational drug design needs to find the best compromise between accuracy and speed, usually in favor of the latter. For several years, this has prevented the widespread use of QM in drug design. Recently, however, hardware has become far more powerful, there has been an increasing development of parallel computing, and QM software has become more sophisticated

and efficiently implemented in quantum chemistry packages. This has led to significant progress in both the modeling of enzyme reactions and the determination of electronic features of the catalytic sites of therapeutically relevant biomolecules. In particular, we are seeing the real possibility of exploiting QM methods in rational drug design, for instance rationalizing subtle information about TS electronic structure or active site polarization effects derived from reaction mechanism studies. However, such instances are scarcely present in the literature, because, in our opinion, it is far from simple to convert outcomes of QM calculations, such as active site polarization or TS electron density, into a real new chemical entity that has the potential to become a drug.

Furthermore, virtual screening (VS),<sup>231</sup> which is an established computational method for discovering new hit compounds, is still far from benefiting from QM methods, as this approach to drug discovery is carried out at a very low level of accuracy, with speed being the dominant parameter in the protocol setting. It might be advanced that this is one of the reasons for the low rate of success of VS in providing new hit compounds. As a matter of fact, we believe that, in this field too, computational drug design could benefit from QM calculations, for instance, in the case of scoring functions and protein active site dynamics, as we have proposed in this review. QM methods could probably help in providing more accurate outcomes of VS simulations when compared to those currently achieved. In this context, a real breakthrough in computational drug design has been the development of efficient and accurate QM/MM schemes that allow one to describe quantum chemical phenomena localized in a target active or binding site, while treating at the MM level the rest of the macromolecule and the solvent. Since this approach makes it possible to investigate biological systems of relatively large dimensions, we believe that QM/MM calculations will play an increasingly prominent role in the future of computational drug design. Indeed, the very recent work of Gräter et al., in which the authors calculated binding affinities for flexible ligands at the QM/MM-PB/SA level of theory, has shown that mixed QM/MM approaches are promising new avenues for drug design based on docking and scoring of small organic molecules at the active site of the biological counterpart.<sup>232</sup>

However, even using QM/MM approaches, only a small fraction of the overall biological complexity may be captured, as all the studies presented here focus to a large extent on a single protein. Biological systems depend on a huge number of molecular interactions that generate an extremely complex network. Examples thereof are the interactions occurring among macromolecules in cells and bringing proteins to interact with each other to reach their own ground states.<sup>233</sup> While advances in genomic research allow one to treat complex biological systems at a highly detailed level, QM studies still use a reductionist approach. Indeed, QM calculations, despite allowing a highly accurate description of atomistic events, can be employed only on small systems. Thus, on one side, we are faced with an overload of information (from genomics and proteomics), which requires connections to be drawn among loosely detailed molecular objects. On the other side, accurate theories are applied to describe a very small fraction of the overall biological complexity. Tackling these problems is not only a matter of computer power; it also calls for a new way of thinking about computational biology.<sup>234</sup> A step in this direction is the recent study on aspartyl proteases, which uses DFT and classical

MD approaches on one single protein and then extends the findings to the entire class of proteins, complementing the quantum chemistry calculations with coarse-grained approaches and structural bioinformatics techniques.<sup>235</sup>

Finally, to cast the development of the application of QM methods in an overall perspective on biological systems modeling, we report an early and illuminating remark of Wimmer, who in 1988 described the role of DFT in the “future” of computational molecular design.<sup>236</sup> Concerning complex systems and reductionism, he wrote: “We are currently witnessing the creation of a new branch of science: the computational approach is establishing itself as a truly new discipline besides the traditional branches of experimentation and theoretical/analytical theory. [...] The goal of all these efforts is a quantitative simulation of complex ‘real world’ systems in terms of encompassing more and more of the environment. This goal is fundamentally different from the analytic approach that tries to isolate, decompose, and idealize systems. The computational approach is synthetic in nature: the goal is the simulation of a complex system and the study of its behavior in a realistic environment.”

## 5. Abbreviations

### Glossary

ACh	acetylcholine
AChBP	acetylcholine binding protein
AChE	acetylcholinesterase
AIDS	acquired immune deficiency syndrome
AM1	Austin Model 1 (a semiempirical method)
B3LYP	hybrid exchange-correlation functional consisting of 20% Hartree–Fock and 80% Becke88 exchange combined with the Lee–Yang–Parr correlation functional
BChE	butyrylcholinesterase
BLYP	exchange-correlation functional consisting of Becke88 exchange combined with the Lee–Yang–Parr correlation functional
CPMD	Car–Parrinello molecular dynamics
CPU	central processing unit (i.e., processor)
DHF	7,8-dihydrofolate
DHFR	dihydrofolate reductase
DFT	density functional theory
EVB	empirical valence bond
fas-2	fasciculin-2
FDA	Food and Drug Administration
GGA	generalized gradient approximation
GTP	guanosine triphosphate
HEPES	<i>N</i> -2-hydroxyethylpiperazine- <i>N</i> -9-(2-ethanesulfonic acid)
HF	Hartree–Fock
HIV-1	human immunodeficiency virus 1
HOMO	highest occupied molecular orbital
KS	Kohn–Sham
LBHB	low barrier hydrogen bond
LDA	local density approximation
LUMO	lowest occupied molecular orbital
LYP	Lee, Yang, and Parr parametrization for the correlation term
MD	molecular dynamics
MFCC	molecular fractionation with conjugate caps
MM	molecular mechanics
MP	Møller–Plesset
MP2	a second-order Møller–Plesset
nACh	nicotinic acetylcholine
NADPH	nicotinamide adenine dinucleotide phosphate (reduced form)

NADP <sup>+</sup>	nicotinamide adenine dinucleotide phosphate (oxidated form)
NMR	nuclear magnetic resonance
P450	cytochrome P450
PBP	penicillin binding protein
PB/SA	Poisson–Boltzmann/surface area continuum solvation model
PDB	protein data bank
PES	potential energy surface
PM3	parametric model number 3 (a semiempirical method)
PW86	Perdew and Wang parametrization for the exchange term dated back to 1986
PW91	Perdew and Wang parametrization for the exchange term dated back to 1991
QM	quantum mechanics
QM/MM	hybrid method that combines quantum mechanics and molecular mechanics: the QM can be DFT (DFT/MM)
QSAR	quantitative structure–activity relationship (when three-dimensional, 3D QSAR)
SAR	structure–activity relationship
TCA	thiazolidinecarboxylic acid
THF	5,6,7,8-tetrahydrofolate
TMIII	transmembrane helix III of a G-protein coupled receptor
TS	transition state
VMD	visual molecular dynamics
VS	virtual screening

## 6. Acknowledgments

MIUR-COFIN, FIRB, and INFM are gratefully acknowledged for their financial support.

## 7. References

- Bohm, H. J.; Klebe, G. *Angew. Chem., Int. Ed.* **1996**, *35*, 2589.
- Jorgensen, W. L. *Science* **2004**, *303*, 1813.
- Sherwood, P. *Methods and algorithms of quantum chemistry*; John von Neumann Institute for Computing: Juelich, 2000; Vol. 1.
- Höltje, H. D.; Höltje, M. In *Quantum Medicinal Chemistry*; Carloni, P., Alber, F., Eds.; Wiley-VCH: Weinheim, Germany, 2003.
- Bader, R. F. W.; Matta, C. F.; Martin, F. J. In *Quantum Medicinal Chemistry*; Carloni, P., Alber, F., Eds.; Wiley-VCH: Weinheim, Germany, 2003.
- Waller, C. L.; Marshall, G. R. *J. Med. Chem.* **1993**, *36*, 2390.
- Oprea, T. I.; Waller, C. L.; Marshall, G. R. *J. Med. Chem.* **1994**, *37*, 2206.
- Singh, P. P.; Srivastava, H. K.; Pasha, F. A. *Bioorg. Med. Chem.* **2004**, *12*, 171.
- Lepp, Z.; Chuman, H. *Bioorg. Med. Chem.* **2005**, *13*, 3093.
- Occhiato, E. G.; Ferrali, A.; Menchi, G.; Guarna, A.; Danza, G.; Comerci, A.; Mancina, R.; Serio, M.; Garotta, G.; Cavalli, A.; De Vivo, M.; Recanatini, M. *J. Med. Chem.* **2004**, *47*, 3546.
- Aguirre, G.; Boiani, L.; Boiani, M.; Cerecetto, H.; Maio, R. D.; Gonzalez, M.; Porcal, W.; Denicola, A.; Piro, O. E.; Castellano, E. E.; Sant'anna, C. M.; Barreiro, E. J. *Bioorg. Med. Chem.* **2005**, *13*, 6336.
- Yamagami, C.; Motohashi, N.; Akamatsu, M. *Bioorg. Med. Chem. Lett.* **2002**, *12*, 2281.
- Wan, J.; Zhang, L.; Yang, G.; Zhan, C. G. *J. Chem. Inf. Comput. Sci.* **2004**, *44*, 2099.
- Carbo, R.; Besalu, E.; Amat, L.; Fradera, X. *J. Math. Chem.* **1995**, *18*, 37.
- Besalu, E.; Girones, X.; Amat, L.; Carbo-Dorca, R. *Acc. Chem. Res.* **2002**, *35*, 289.
- Banci, L.; Schroder, S.; Kollman, P. A. *Proteins* **1992**, *13*, 288.
- Cavalli, A.; Dezi, C.; Folkers, G.; Scapozza, L.; Recanatini, M. *Proteins* **2001**, *45*, 478.
- Gogonea, V.; Suarez, D.; van der Vaart, A.; Merz, K. M., Jr. *Curr. Opin. Struct. Biol.* **2001**, *11*, 217.
- Garcia-Viloca, M.; Gao, J.; Karplus, M.; Truhlar, D. G. *Science* **2004**, *303*, 186.
- Schramm, V. L. *Annu. Rev. Biochem.* **1998**, *67*, 693.
- Schramm, V. L. *Arch. Biochem. Biophys.* **2005**, *433*, 13.
- Sulpizi, M.; Schelling, P.; Folkers, G.; Carloni, P.; Scapozza, L. *J. Biol. Chem.* **2001**, *276*, 21692.
- Sandala, G. M.; Smith, D. M.; Radom, L. *J. Am. Chem. Soc.* **2005**, *127*, 8856.
- Villar, R.; Gil, M. J.; Garcia, J. I.; Martinez-Merino, V. *J. Comput. Chem.* **2005**, *26*, 1347.
- Koch, W.; Holthausen, M. C. *A chemist's guide to density functional theory*; Wiley-VCH: Weinheim, Germany, 2001.
- Cavalli, A., Ed. *Quant. Struct.–Act. Relat.* **2002**, *21*.
- Quantum Medicinal Chemistry*; Carloni, P., Alber, F., Ed.; Wiley-VCH: Weinheim, Germany, 2003.
- von Lilienfeld, O. A.; Lins, R. D.; Röthlisberger, U. *Phys. Rev. Lett.* **2005**, *95*, 153002.
- Waller, M. P.; Robertazzi, A.; Platts, J. A.; Hibbs, D. E.; Williams, P. A. *J. Comput. Chem.* **2006**, *27*, 491.
- Karplus, M. *Acc. Chem. Res.* **2002**, *35*, 321.
- Karplus, M.; McCammon, J. A. *Nat. Struct. Biol.* **2002**, *9*, 646.
- Car, R.; Parrinello, M. *Phys. Rev. Lett.* **1985**, *55*, 2471.
- Aqvist, J.; Warshel, A. *Chem. Rev.* **1993**, *93*, 2523.
- Combined quantum mechanical and molecular mechanical methods*; Gao, J., Thompson, M. A., Eds.; American Chemical Society: Washington, DC, 1998.
- Warshel, A. *Annu. Rev. Biophys. Biomol. Struct.* **2003**, *32*, 425.
- Laio, A.; VandeVondele, J.; Röthlisberger, U. *J. Chem. Phys.* **2002**, *116*, 6941.
- Laio, A.; VandeVondele, J.; Röthlisberger, U. *J. Phys. Chem. B* **2002**, *106*, 7300.
- Eichinger, M.; Tavan, P.; Hutter, J.; Parrinello, M. *J. Chem. Phys.* **1999**, *110*, 10452.
- Leach, A. R. In *Molecular modelling. Principles and applications*; Addison-Wesley: Reading, MA, 1996.
- Jensen, F. *Introduction to computational chemistry*; John Wiley and Sons: New York, 1999.
- Cramer, C. J. *Essentials of computational chemistry: theories and models*; John Wiley and Sons: New York, 2004.
- Marx, D.; Hutter, J. In *Modern methods and algorithms of quantum chemistry*; Grotendorst, J., Ed.; John vonNeumann Institute for Computing: Jülich, 2000; Vol. 1.
- Møller, C.; Plesset, M. S. *Phys. Rev.* **1934**, *46*, 618.
- Siegbahn, P. E.; Blomberg, M. R. A. *Chem. Rev.* **2000**, *100*, 421.
- Ghosh, A.; Taylor, P. R. *Curr. Opin. Chem. Biol.* **2003**, *7*, 113.
- Himo, F.; Siegbahn, P. E. *Chem. Rev.* **2003**, *103*, 2421.
- Hohenberg, P.; Kohn, W. *Phys. Rev.* **1964**, *136*, B864.
- Kohn, W.; Sham, L. J. *Phys. Rev.* **1965**, *140*, A1133.
- Becke, A. D. *Phys. Rev. A* **1988**, *38*, 3098.
- Perdew, J. P.; Wang, Y. *Phys. Rev. B* **1986**, *33*, 8800.
- Perdew, J. P.; Wang, Y. *Phys. Rev. B* **1992**, *45*, 13244.
- Lee, C. T.; Yang, W. T.; Parr, R. G. *Phys. Rev. B* **1988**, *37*, 785.
- Becke, A. D. *J. Chem. Phys.* **1993**, *98*, 1372.
- Curtiss, L. A.; Raghavachari, K.; Redfern, P. C.; Pople, J. A. *J. Chem. Phys.* **2000**, *112*, 7374.
- Remler, D. K.; Madden, P. A. *Mol. Phys.* **1990**, *70*, 921.
- Payne, M. C.; Teter, M. P.; Allan, D. C.; Arias, T. A.; Joannopoulos, J. D. *Rev. Mod. Phys.* **1992**, *64*, 1045.
- Warshel, A.; Levitt, M. *J. Mol. Biol.* **1976**, *103*, 227.
- Truhlar, D. G.; Gao, J.; Alhambra, C.; Garcia-Viloca, M.; Corchado, J.; Sanchez, M. L.; Villa, J. *Acc. Chem. Res.* **2002**, *35*, 341.
- Schlegel, H. B. *J. Comput. Chem.* **2003**, *24*, 1514.
- Kohen, A.; Klinman, J. P. *Acc. Chem. Res.* **1998**, *31*, 397.
- Kohen, A.; Klinman, J. P. *Chem. Biol.* **1999**, *6*, R191.
- Car, R. *Quant. Struct.–Act. Relat.* **2002**, *21*, 97.
- Bruice, T. C.; Kahn, K. *Curr. Opin. Chem. Biol.* **2000**, *4*, 540.
- Friesner, R. A.; Dunietz, B. D. *Acc. Chem. Res.* **2001**, *34*, 351.
- Gao, J.; Truhlar, D. G. *Annu. Rev. Phys. Chem.* **2002**, *53*, 467.
- Ridder, L.; Mulholland, A. J. *Curr. Top. Med. Chem.* **2003**, *3*, 1241.
- Benkovic, S. J.; Hammes-Schiffer, S. *Science* **2003**, *301*, 1196.
- Marti, S.; Roca, M.; Andres, J.; Moliner, V.; Silla, E.; Tunon, I.; Bertran, J. *Chem. Soc. Rev.* **2004**, *33*, 98.
- Friesner, R. A.; Guallar, V. *Annu. Rev. Phys. Chem.* **2005**, *56*, 389.
- Ryde, U. *Curr. Opin. Chem. Biol.* **2003**, *7*, 136.
- Cleland, W. W.; Frey, P. A.; Gerlt, J. A. *J. Biol. Chem.* **1998**, *273*, 25529.
- Dougherty, D. A. *Science* **1996**, *271*, 163.
- Ma, J. C.; Dougherty, D. A. *Chem. Rev.* **1997**, *97*, 1303.
- Masgrau, L.; Roujeinikova, A.; Johannissen, L. O.; Hothi, P.; Basran, J.; Ranaghan, K. E.; Mulholland, A. J.; Sutcliffe, M. J.; Scrutton, N. S.; Leys, D. *Science* **2006**, *312*, 237.
- Loew, G. H.; Harris, D. L. *Chem. Rev.* **2000**, *100*, 407.
- Segall, M. D. *J. Phys.: Condens. Matter* **2002**, *14*, 2957.
- Meunier, B.; de Visser, S. P.; Shaik, S. *Chem. Rev.* **2004**, *104*, 3947.
- Shaik, S.; Kumar, D.; de Visser, S. P.; Altun, A.; Thiel, W. *Chem. Rev.* **2005**, *105*, 2279.
- Harris, D. L. *Curr. Opin. Drug Discovery Dev.* **2004**, *7*, 43.
- Harris, D. L.; Park, J. Y.; Gruenke, L.; Waskell, L. *Proteins* **2004**, *55*, 895.

- (81) Puente, X. S.; Sanchez, L. M.; Overall, C. M.; Lopez-Otin, C. *Nat. Rev. Genet.* **2003**, *4*, 544.
- (82) Tyndall, J. D.; Nall, T.; Fairlie, D. P. *Chem. Rev.* **2005**, *105*, 973.
- (83) Piana, S.; Sebastiani, D.; Carloni, P.; Parrinello, M. *J. Am. Chem. Soc.* **2001**, *123*, 8730.
- (84) Piana, S.; Carloni, P.; Röthlisberger, U. *Protein Sci.* **2002**, *11*, 2393.
- (85) Piana, S.; Carloni, P.; Parrinello, M. *J. Mol. Biol.* **2002**, *319*, 567.
- (86) Piana, S.; Bucher, D.; Carloni, P.; Röthlisberger, U. *J. Phys. Chem. B* **2004**, *108*, 11139.
- (87) Carloni, P. *Quant. Struct.–Act. Relat.* **2002**, *21*, 166.
- (88) Sirois, S.; Proynov, E. I.; Truchon, J. F.; Tsoukas, C. M.; Salahub, D. R. *J. Comput. Chem.* **2003**, *24*, 1110.
- (89) Wlodawer, A.; Erickson, J. W. *Annu. Rev. Biochem.* **1993**, *62*, 543.
- (90) Wlodawer, A.; Vondrasek, J. *Annu. Rev. Biophys. Biomol. Struct.* **1998**, *27*, 249.
- (91) Kempf, D. J.; Codacovi, L.; Wang, X. C.; Kohlbrenner, W. E.; Wideburg, N. E.; Saldivar, A.; Vasavanonda, S.; Marsh, K. C.; Bryant, P.; Sham, H. L.; et al. *J. Med. Chem.* **1993**, *36*, 320.
- (92) Curioni, A.; Mordasini, T.; Andreoni, W. *J. Comput.-Aided Mol. Des.* **2004**, *18*, 773.
- (93) Raha, K.; Merz, K. M., Jr. *J. Med. Chem.* **2005**, *48*, 4558.
- (94) Zhang, D. W.; Zhang, J. Z. H. *J. Chem. Phys.* **2003**, *119*, 3599.
- (95) Zhang, D. W.; Xiang, Y.; Zhang, J. Z. H. *J. Phys. Chem. B* **2003**, *107*, 12039.
- (96) Nivesanonond, K.; Peeter, A.; Lamoen, D.; Van Alsenoy, C. *Int. J. Quantum Chem.* **2005**, *105*, 292.
- (97) Powers, J. C.; Asgian, J. L.; Ekici, O. D.; James, K. E. *Chem. Rev.* **2002**, *102*, 4639.
- (98) Ishida, T.; Kato, S. *J. Am. Chem. Soc.* **2003**, *125*, 12035.
- (99) Topf, M.; Richards, W. G. *J. Am. Chem. Soc.* **2004**, *126*, 14631.
- (100) Nemukhin, A. V.; Grigorenko, B. L.; Rogov, A. V.; Topol, I. A.; Burt, S. K. *Theor. Chem. Acc.* **2004**, *111*, 36.
- (101) Gordon, M. S.; Freitag, M. A.; Bandyopadhyay, P.; Jensen, J. H.; Kairys, V.; Stevens, W. J. *J. Phys. Chem. A* **2001**, *105*, 293.
- (102) Pearson, N. D.; Eggleston, D. S.; Haltiwanger, R. C.; Hibbs, M.; Laver, A. J.; Kaura, A. C. *Bioorg. Med. Chem. Lett.* **2002**, *12*, 2359.
- (103) Costanzo, M. J.; Yabut, S. C.; Almond, H. R., Jr.; Andrade-Gordon, P.; Corcoran, T. W.; De Garavilla, L.; Kauffman, J. A.; Abraham, W. M.; Recacha, R.; Chattopadhyay, D.; Maryanoff, B. E. *J. Med. Chem.* **2003**, *46*, 3865.
- (104) Hansen, K. K.; Grosch, B.; Greiveldinger-Poenu, S.; Bartlett, P. A. *J. Org. Chem.* **2003**, *68*, 8465.
- (105) Smyth, T. P. *Bioorg. Med. Chem.* **2004**, *12*, 4081.
- (106) Recanatini, M.; Valenti, P. *Curr. Pharm. Des.* **2004**, *10*, 3157.
- (107) Giacobini, E. *Pharmacol. Res.* **2004**, *50*, 433.
- (108) Pan, Y.; Gao, D.; Yang, W.; Cho, H.; Yang, G.; Tai, H. H.; Zhan, C. G. *Proc. Natl. Acad. Sci., U.S.A.* **2005**, *102*, 16656.
- (109) Quinn, D. M. *Chem. Rev.* **1987**, *87*, 955.
- (110) Lane, R. M.; Kivipelto, M.; Greig, N. H. *Clin. Neuropharmacol.* **2004**, *27*, 141.
- (111) Hölting, H. D.; Kier, L. B. *J. Pharm. Sci.* **1975**, *64*, 418.
- (112) Shen, T.; Tai, K.; Henchman, R. H.; McCammon, J. A. *Acc. Chem. Res.* **2002**, *35*, 332.
- (113) Zhang, Y.; Kua, J.; McCammon, J. A. *J. Am. Chem. Soc.* **2002**, *124*, 10572.
- (114) Zhang, Y.; Kua, J.; McCammon, J. A. *J. Phys. Chem. B* **2003**, *107*, 4459.
- (115) Wang, J.; Gu, J.; Leszczynski, J. *J. Phys. Chem. B* **2005**, *109*, 13761.
- (116) Kitaura, K.; Morokuma, K. *Int. J. Quantum Chem.* **1976**, *10*, 325.
- (117) De Ferrari, G. V.; Canales, M. A.; Shin, I.; Weiner, L. M.; Silman, I.; Inestrosa, N. C. *Biochemistry* **2001**, *40*, 10447.
- (118) Zhan, C. G.; Gao, D. *Biophys. J.* **2005**, *89*, 3863.
- (119) Cornell, W. D.; Cieplak, P.; Bayly, C. I.; Gould, I. R.; Merz, K. M.; Ferguson, D. M.; Spellmeyer, D. C.; Fox, T.; Caldwell, J. W.; Kollman, P. A. *J. Am. Chem. Soc.* **1995**, *117*, 5179.
- (120) Gao, D.; Cho, H.; Yang, W.; Pan, Y.; Yang, G.; Tai, H. H.; Zhan, C. G. *Angew. Chem., Int. Ed.* **2006**, *45*, 653.
- (121) Cleland, W. W. *Biochemistry* **1992**, *31*, 317.
- (122) Cleland, W. W.; Kreevoy, M. M. *Science* **1994**, *264*, 1887.
- (123) Cleland, W. W. *Arch. Biochem. Biophys.* **2000**, *382*, 1.
- (124) Frey, P. A.; Whitt, S. A.; Tobin, J. B. *Science* **1994**, *264*, 1927.
- (125) Tobin, J. B.; Whitt, S. A.; Cassidy, C. S.; Frey, P. A. *Biochemistry* **1995**, *34*, 6919.
- (126) Cassidy, C. S.; Lin, J.; Frey, P. A. *Biochemistry* **1997**, *36*, 4576.
- (127) Lin, J.; Cassidy, C. S.; Frey, P. A. *Biochemistry* **1998**, *37*, 11940.
- (128) Lin, J.; Westler, W. M.; Cleland, W. W.; Markley, J. L.; Frey, P. A. *Proc. Natl. Acad. Sci., U.S.A.* **1998**, *95*, 14664.
- (129) Neidhart, D.; Wei, Y.; Cassidy, C.; Lin, J.; Cleland, W. W.; Frey, P. A. *Biochemistry* **2001**, *40*, 2439.
- (130) Westler, W. M.; Frey, P. A.; Lin, J.; Wemmer, D. E.; Morimoto, H.; Williams, P. G.; Markley, J. L. *J. Am. Chem. Soc.* **2002**, *124*, 4196.
- (131) Ishida, T.; Kato, S. *J. Am. Chem. Soc.* **2004**, *126*, 7111.
- (132) Topf, M.; Varnai, P.; Richards, W. G. *J. Am. Chem. Soc.* **2002**, *124*, 14780.
- (133) Ash, E. L.; Sudmeier, J. L.; De Fabo, E. C.; Bachovchin, W. W. *Science* **1997**, *278*, 1128.
- (134) Otto, H.-H.; Schirmeister, T. *Chem. Rev.* **1997**, *97*, 133.
- (135) Denault, J. B.; Salvesen, G. S. *Chem. Rev.* **2002**, *102*, 4489.
- (136) Lecaille, F.; Kaleta, J.; Bromme, D. *Chem. Rev.* **2002**, *102*, 4459.
- (137) Sulpizi, M.; Laio, A.; VandeVondele, J.; Cattaneo, A.; Röthlisberger, U.; Carloni, P. *Proteins* **2003**, *52*, 212.
- (138) Dellago, C.; Bolhuis, P. G.; Chandler, D. *J. Chem. Phys.* **1999**, *119*, 6617.
- (139) Gregersen, B. A.; Lopez, X.; York, D. M. *J. Am. Chem. Soc.* **2003**, *125*, 7178.
- (140) Helten, H.; Schirmeister, T.; Engels, B. *J. Org. Chem.* **2005**, *70*, 233.
- (141) Walsh, C. *Nature* **2000**, *406*, 775.
- (142) van Heijenoort, J. *Glycobiology* **2001**, *11*, 25R.
- (143) Neu, H. C. *Science* **1992**, *257*, 1064.
- (144) Cohen, M. L. *Science* **1992**, *257*, 1050.
- (145) Davies, J. *Science* **1994**, *264*, 375.
- (146) Bush, K.; Jacoby, G. A.; Medeiros, A. A. *Antimicrob. Agents Chemother.* **1995**, *39*, 1211.
- (147) Massova, I.; Kollman, P. A. *J. Comput. Chem.* **2002**, *23*, 1559.
- (148) Field, M. J.; Bash, P. A.; Karplus, M. *J. Comput. Chem.* **1990**, *11*, 700.
- (149) Hermann, J. C.; Ridder, L.; Mulholland, A. J.; Hölting, H. D. *J. Am. Chem. Soc.* **2003**, *125*, 9590.
- (150) Hermann, J. C.; Hensen, C.; Ridder, L.; Mulholland, A. J.; Hölting, H. D. *J. Am. Chem. Soc.* **2005**, *127*, 4454.
- (151) Meroueh, S. O.; Fisher, J. F.; Schlegel, H. B.; Mobashery, S. *J. Am. Chem. Soc.* **2005**, *127*, 15397.
- (152) Gherman, B. F.; Goldberg, S. D.; Cornish, V. W.; Friesner, R. A. *J. Am. Chem. Soc.* **2004**, *126*, 7652.
- (153) Schrodinger Inc.: Portland, OR, 2000.
- (154) Jorgensen, W. L.; Maxwell, D. S.; Tirado-Rives, J. *J. Am. Chem. Soc.* **1996**, *118*, 11225.
- (155) Hata, M.; Tanaka, Y.; Fujii, Y.; Neya, S.; Hoshino, T. *J. Phys. Chem. B* **2005**, *109*, 16153.
- (156) Cricco, J. A.; Vila, A. J. *Curr. Pharm. Des.* **1999**, *5*, 915.
- (157) Tomatis, P. E.; Rasia, R. M.; Segovia, L.; Vila, A. J. *Proc. Natl. Acad. Sci., U.S.A.* **2005**, *102*, 13761.
- (158) Diaz, N.; Suarez, D.; Merz, K. M., Jr. *J. Am. Chem. Soc.* **2001**, *123*, 9867.
- (159) Suarez, D.; Brothers, E. N.; Merz, K. M., Jr. *Biochemistry* **2002**, *41*, 6615.
- (160) Dal Peraro, M.; Vila, A. J.; Carloni, P. *J. Biol. Inorg. Chem.* **2002**, *7*, 704.
- (161) Dal Peraro, M.; Vila, A. J.; Carloni, P. *Inorg. Chem.* **2003**, *42*, 4245.
- (162) Dal Peraro, M.; Llarrull, L. I.; Röthlisberger, U.; Vila, A. J.; Carloni, P. *J. Am. Chem. Soc.* **2004**, *126*, 12661.
- (163) Gaussian Inc.: Pittsburgh, PA, 1998.
- (164) Park, H.; Brothers, E. N.; Merz, K. M., Jr. *J. Am. Chem. Soc.* **2005**, *127*, 4232.
- (165) Olsen, L.; Rasmussen, T.; Hemmingsen, L.; Ryde, U. *J. Phys. Chem. B* **2004**, *108*, 17639.
- (166) Morris, G. M.; Goodsell, D. S.; Halliday, R. S.; Huey, R.; Hart, W. E.; Belew, R. K.; Olson, A. J. *J. Comput. Chem.* **1998**, *19*, 1639.
- (167) Xu, D.; Zhou, Y.; Xie, D.; Guo, H. *J. Med. Chem.* **2005**, *48*, 6679.
- (168) Garau, G.; Bebrone, C.; Anne, C.; Galleni, M.; Frere, J. M.; Dideberg, O. *J. Mol. Biol.* **2005**, *345*, 785.
- (169) Elstner, M.; Porezag, D.; Jungnickel, G.; Elsner, J.; Haugk, M.; Frauenheim, T.; Suhai, S.; Seifert, G. *Phys. Rev. B* **1998**, *58*, 7260.
- (170) Schnell, J. R.; Dyson, H. J.; Wright, P. E. *Annu. Rev. Biophys. Biomol. Struct.* **2004**, *33*, 119.
- (171) Miller, G. P.; Benkovic, S. J. *Chem. Biol.* **1998**, *5*, R105.
- (172) Kisliuk, R. L. *Curr. Pharm. Des.* **2003**, *9*, 2615.
- (173) Then, R. L. *J. Chemother.* **2004**, *16*, 3.
- (174) Brady, R. L.; Cameron, A. *Curr. Drug Targets* **2004**, *5*, 137.
- (175) Fierke, C. A.; Johnson, K. A.; Benkovic, S. J. *Biochemistry* **1987**, *26*, 4085.
- (176) Stone, S. R.; Morrison, J. F. *Biochemistry* **1988**, *27*, 5493.
- (177) Morrison, J. F.; Stone, S. R. *Biochemistry* **1988**, *27*, 5499.
- (178) Cummins, P. L.; Gready, J. E. *J. Am. Chem. Soc.* **2001**, *123*, 3418.
- (179) Cummins, P. L.; Greatbanks, S. P.; Rendell, A. P.; Gready, J. E. *J. Phys. Chem. B* **2002**, *106*, 9934.
- (180) Shrimpton, P.; Mullaney, A.; Allemann, R. K. *Proteins* **2003**, *51*, 216.
- (181) Shrimpton, P.; Allemann, R. K. *Protein Sci.* **2002**, *11*, 1442.
- (182) Garcia-Viloca, M.; Truhlar, D. G.; Gao, J. *Biochemistry* **2003**, *42*, 13558.
- (183) Agarwal, P. K.; Billeter, S. R.; Hammes-Schiffer, S. *J. Phys. Chem. B* **2002**, *106*, 3283.
- (184) Pu, J.; Ma, S.; Garcia-Viloca, M.; Gao, J.; Truhlar, D. G.; Kohen, A. *J. Am. Chem. Soc.* **2005**, *127*, 14879.

- (185) Gronert, S.; Keeffe, J. R. *J. Am. Chem. Soc.* **2005**, *127*, 2324.
- (186) Pu, J.; Ma, S.; Gao, J.; Truhlar, D. G. *J. Phys. Chem. B* **2005**, *109*, 8551.
- (187) Hammes-Schiffer, S. *Curr. Opin. Struct. Biol.* **2004**, *14*, 192.
- (188) Truhlar, D. G. In *Isotope effects in chemistry and biology*; Kohlen, A.; Limbach, H. H., Eds.; Taylor & Francis Group, CRC Press: New York, 2005; Vol. 22.
- (189) Garcia-Viloca, M.; Truhlar, D. G.; Gao, J. *J. Mol. Biol.* **2003**, *327*, 549.
- (190) Mecozzi, S.; West, A. P., Jr.; Dougherty, D. A. *Proc. Natl. Acad. Sci., U.S.A.* **1996**, *93*, 10566.
- (191) Sunner, J.; Nishizawa, K.; Kebarle, P. *J. Phys. Chem.* **1981**, *85*, 1814.
- (192) Caldwell, J. W.; Kollman, P. A. *J. Am. Chem. Soc.* **1995**, *117*, 4177.
- (193) Branduardi, D.; Gervasio, F. L.; Cavalli, A.; Recanatini, M.; Parrinello, M. *J. Am. Chem. Soc.* **2005**, *127*, 9147.
- (194) Laio, A.; Parrinello, M. *Proc. Natl. Acad. Sci., U.S.A.* **2002**, *99*, 12562.
- (195) Mo, Y.; Subramanian, G.; Gao, J.; Ferguson, D. M. *J. Am. Chem. Soc.* **2002**, *124*, 4832.
- (196) Moro, S.; Spalluto, G.; Jacobson, K. A. *Trends Pharmacol. Sci.* **2005**, *26*, 44.
- (197) Fanelli, F.; De Benedetti, P. G. *Chem. Rev.* **2005**, *105*, 3297.
- (198) Palczewski, K.; Kumasaka, T.; Hori, T.; Behnke, C. A.; Motoshima, H.; Fox, B. A.; Le Trong, I.; Teller, D. C.; Okada, T.; Stenkamp, R. E.; Yamamoto, M.; Miyano, M. *Science* **2000**, *289*, 739.
- (199) Befort, K.; Zilliox, C.; Filliol, D.; Yue, S.; Kieffer, B. L. *J. Biol. Chem.* **1999**, *274*, 18574.
- (200) Befort, K.; Tabbara, L.; Kling, D.; Maignet, B.; Kieffer, B. L. *J. Biol. Chem.* **1996**, *271*, 10161.
- (201) Mo, Y.; Peyerimhoff, S. D. *J. Chem. Phys.* **1998**, *109*, 1687.
- (202) Schmidt, M. W.; Baldridge, K. K.; Boatz, J. A.; Elbert, S. T.; Gordon, M. S.; Jensen, J. H.; Koseki, S.; Matsunaga, N.; Nguyen, K. A.; Su, S. J.; Windus, T. L.; Dupuis, M.; Montgomery, J. A. *J. Comput. Chem.* **1993**, *14*, 1347.
- (203) Gallivan, J. P.; Dougherty, D. A. *J. Am. Chem. Soc.* **2000**, *122*, 870.
- (204) Romanelli, M. N.; Gualtieri, F. *Med. Res. Rev.* **2003**, *23*, 393.
- (205) Holladay, M. W.; Dart, M. J.; Lynch, J. K. *J. Med. Chem.* **1997**, *40*, 4169.
- (206) Smit, A. B.; Syed, N. I.; Schaap, D.; van Minnen, J.; Klumperman, J.; Kits, K. S.; Lodder, H.; van der Schors, R. C.; van Elk, R.; Sorgedrager, B.; Brejc, K.; Sixma, T. K.; Geraerts, W. P. *Nature* **2001**, *411*, 261.
- (207) Celie, P. H.; van Rossum-Fikkert, S. E.; van Dijk, W. J.; Brejc, K.; Smit, A. B.; Sixma, T. K. *Neuron* **2004**, *41*, 907.
- (208) Le Novere, N.; Grutter, T.; Changeux, J. P. *Proc. Natl. Acad. Sci., U.S.A.* **2002**, *99*, 3210.
- (209) Costa, V.; Nistri, A.; Cavalli, A.; Carloni, P. *Br. J. Pharmacol.* **2003**, *140*, 921.
- (210) Huang, X.; Zheng, F.; Crooks, P. A.; Dvoskin, L. P.; Zhan, C. G. *J. Am. Chem. Soc.* **2005**, *127*, 14401.
- (211) Cashin, A. L.; Petersson, E. J.; Lester, H. A.; Dougherty, D. A. *J. Am. Chem. Soc.* **2005**, *127*, 350.
- (212) Beene, D. L.; Brandt, G. S.; Zhong, W.; Zacharias, N. M.; Lester, H. A.; Dougherty, D. A. *Biochemistry* **2002**, *41*, 10262.
- (213) Morreale, A.; Maseras, F.; Iriepa, I.; Galvez, E. *J. Mol. Graphics Modell.* **2002**, *21*, 111.
- (214) Galvez-Ruano, E.; Iriepa-Canada, I.; Morreale, A.; Lipkowitz, K. B. *J. Comput.-Aided Mol. Des.* **1999**, *13*, 57.
- (215) Bouzat, C.; Gumilar, F.; Spitzmaul, G.; Wang, H. L.; Rayes, D.; Hansen, S. B.; Taylor, P.; Sine, S. M. *Nature* **2004**, *430*, 896.
- (216) Giorgetti, A.; Carloni, P. *Curr. Opin. Chem. Biol.* **2003**, *7*, 150.
- (217) Martens, J. R.; O'Connell, K.; Tamkun, M. *Trends Pharmacol. Sci.* **2004**, *25*, 16.
- (218) Doyle, D. A.; Morais Cabral, J.; Pfuetzner, R. A.; Kuo, A.; Gulbis, J. M.; Cohen, S. L.; Chait, B. T.; MacKinnon, R. *Science* **1998**, *280*, 69.
- (219) Morais Cabral, J. H.; Lee, A.; Cohen, S. L.; Chait, B. T.; Li, M.; MacKinnon, R. *Cell* **1998**, *95*, 649.
- (220) Jiang, Y.; Lee, A.; Chen, J.; Cadene, M.; Chait, B. T.; MacKinnon, R. *Nature* **2002**, *417*, 515.
- (221) Dutzler, R.; Campbell, E. B.; Cadene, M.; Chait, B. T.; MacKinnon, R. *Nature* **2002**, *415*, 287.
- (222) Jiang, Y.; Lee, A.; Chen, J.; Ruta, V.; Cadene, M.; Chait, B. T.; MacKinnon, R. *Nature* **2003**, *423*, 33.
- (223) Long, S. B.; Campbell, E. B.; MacKinnon, R. *Science* **2005**, *309*, 897.
- (224) Guidoni, L.; Carloni, P. *Biochim. Biophys. Acta* **2002**, *1563*, 1.
- (225) Munoz-Caro, C.; Nino, A. *Biophys. Chem.* **2002**, *96*, 1.
- (226) Ban, F.; Kusalik, P.; Weaver, D. F. *J. Am. Chem. Soc.* **2004**, *126*, 4711.
- (227) De Ponti, F.; Poluzzi, E.; Cavalli, A.; Recanatini, M.; Montanaro, N. *Drug Saf.* **2002**, *25*, 263.
- (228) Pearlstein, R.; Vaz, R.; Rampe, D. *J. Med. Chem.* **2003**, *46*, 2017.
- (229) Recanatini, M.; Cavalli, A.; Masetti, M. *Novartis Found. Symp.* **2005**, *266*, 171–81; discussion 181.
- (230) Recanatini, M.; Poluzzi, E.; Masetti, M.; Cavalli, A.; De Ponti, F. *Med. Res. Rev.* **2005**, *25*, 133.
- (231) Shoichet, B. K. *Nature* **2004**, *432*, 862.
- (232) Gräter, F.; Schwarzl, S. M.; Dejaegere, A.; Fischer, S.; Smith, J. C. *J. Phys. Chem. B* **2005**, *109*, 10474.
- (233) Weiss, J. N.; Qu, Z.; Garfinkel, A. *FASEB J.* **2003**, *17*, 1.
- (234) Noble, D. *Nat. Rev. Mol. Cell. Biol.* **2002**, *3*, 459.
- (235) Cascella, M.; Micheletti, C.; Röthlisberger, U.; Carloni, P. *J. Am. Chem. Soc.* **2005**, *127*, 3734.
- (236) Wimmer, E. *J. Comput.-Aided Mol. Des.* **1988**, *1*, 283.
- (237) Hensen, C.; Hermann, J. C.; Nam, K.; Ma, S.; Gao, J.; Höltje, H. D. *J. Med. Chem.* **2004**, *47*, 6673.
- (238) Zhang, D. W.; Zhang, J. Z. H. *Int. J. Quantum Chem.* **2005**, *103*, 2467.
- (239) Vidossich, P.; Carloni, P. *J. Phys. Chem. B* **2006**, *110*, 1437.
- (240) Nemukhin, A. V.; Topol, I. A.; Burt, S. K. *Int. J. Quantum Chem.* **2002**, *88*, 34.
- (241) Schiott, B. *Chem. Commun.* **2004**, 498.
- (242) Shokhen, M.; Albeck, A. *Proteins* **2004**, *54*, 468.
- (243) Tachikawa, H.; Igarashi, M.; Nishihira, J.; Ishibashi, T. *J. Photochem. Photobiol., B* **2005**, *79*, 11.
- (244) Gao, D.; Zhan, C. G. *Proteins* **2006**, *62*, 99.
- (245) Lin, Y. L.; Chang, N. Y.; Lim, C. *J. Am. Chem. Soc.* **2002**, *124*, 12042.
- (246) Fujii, Y.; Hata, M.; Hoshino, T.; Tsuda, M. *J. Phys. Chem. B* **2002**, *106*, 9687.
- (247) Castillo, R.; Silla, E.; Tunon, I. *J. Am. Chem. Soc.* **2002**, *124*, 1809.
- (248) Ke, Y. Y.; Lin, T. H. *Biophys. Chem.* **2005**, *114*, 103.
- (249) Li, J.; Cross, J. B.; Vreven, T.; Meroueh, S. O.; Mobashery, S.; Schlegel, H. B. *Proteins* **2005**, *61*, 246.
- (250) Olsen, L.; Antony, J.; Hemmingsen, L.; Mikkelsen, K. V. *J. Phys. Chem. A* **2002**, *106*, 1046.
- (251) Cummins, P. L.; Greatbanks, S. P.; Rendell, A. P.; Gready, J. E. *J. Phys. Chem. B* **2002**, *106*, 9934.
- (252) Ferrer, S.; Silla, E.; Tunon, I.; Marti, S.; Moliner, V. *J. Phys. Chem. B* **2003**, *107*, 14036.
- (253) Watney, J. B.; Agarwal, P. K.; Hammes-Schiffer, S. *J. Am. Chem. Soc.* **2003**, *125*, 3745.
- (254) Cummins, P. L.; Gready, J. E. *J. Comput. Chem.* **2005**, *26*, 561.
- (255) Wong, K. F.; Selzer, T.; Benkovic, S. J.; Hammes-Schiffer, S. *Proc. Natl. Acad. Sci., U.S.A.* **2005**, *102*, 6807.
- (256) Isaev, A. N. *THEOCHEM* **2002**, *582*, 195.
- (257) Remko, M.; Garaj, V. *Mol. Phys.* **2003**, *101*, 2357.
- (258) Loferer, M. J.; Tautermann, C. S.; Loeffler, H. H.; Liedl, K. R. *J. Am. Chem. Soc.* **2003**, *125*, 8921.
- (259) Tautermann, C. S.; Loferer, M. J.; Voegelé, A. F.; Liedl, K. R. *J. Phys. Chem. B* **2003**, *107*, 12013.
- (260) Garcia-Viloca, M.; Nam, K.; Alhambra, C.; Gao, J. *J. Phys. Chem. B* **2004**, *108*, 13501.
- (261) Bottoni, A.; Lanza, C. Z.; Miscione, G. P.; Spinelli, D. *J. Am. Chem. Soc.* **2004**, *126*, 1542.
- (262) Schenk, S.; Kesselmeier, J.; Anders, E. *Chemistry* **2004**, *10*, 3091.
- (263) Marino, T.; Russo, N.; Toscano, M. *J. Am. Chem. Soc.* **2005**, *127*, 4242.
- (264) Cavalli, A.; De Vivo, M.; Recanatini, M. *Chem. Commun.* **2003**, 1308.
- (265) Duca, J. S.; Madison, V. S. *Biopolymers* **2005**, *80*, 312.
- (266) Fernandes, P. A.; Ramos, M. J. *J. Am. Chem. Soc.* **2003**, *125*, 6311.
- (267) Pelmenchikov, V.; Cho, K. B.; Siegbahn, P. E. *J. Comput. Chem.* **2004**, *25*, 311.
- (268) Cerqueira, N. M. F. S. A.; Fernandes, P. A.; Erickson, L. A.; Romos, M. J. *THEOCHEM* **2004**, *709*, 53.
- (269) Cho, K. B.; Pelmenchikov, V.; Graslund, A.; Siegbahn, P. E. M. *J. Phys. Chem. B* **2004**, *108*, 2056.
- (270) Jorgensen, A. T.; Norrby, P. O.; Liljefors, T. *J. Comput.-Aided Mol. Des.* **2002**, *16*, 167.
- (271) Klein, C. D.; Schiffmann, R.; Folkers, G.; Piana, S.; Röthlisberger, U. *J. Biol. Chem.* **2003**, *278*, 47862.
- (272) Cavalli, A.; Carloni, P. *J. Am. Chem. Soc.* **2002**, *124*, 3763.
- (273) Topol, I. A.; Cachau, R. E.; Nemukhin, A. V.; Grigorenko, B. L.; Burt, S. K. *Biochim. Biophys. Acta* **2004**, *1700*, 125.
- (274) Grigorenko, B. L.; Nemukhin, A. V.; Topol, I. A.; Cachau, R. E.; Burt, S. K. *Proteins* **2005**, *60*, 495.
- (275) Grigorenko, B. L.; Nemukhin, A. V.; Cachau, R. E.; Topol, I. A.; Burt, S. K. *J. Mol. Model.* **2005**, *11*, 503 (online).
- (276) Xiao, X.; Antony, S.; Pommier, Y.; Cushman, M. *J. Med. Chem.* **2005**, *48*, 3231.
- (277) Xiao, X.; Cushman, M. *J. Am. Chem. Soc.* **2005**, *127*, 9960.
- (278) Xiao, X.; Cushman, M. *J. Org. Chem.* **2005**, *70*, 9584.
- (279) Bernardi, F.; Bottoni, A.; De Vivo, M.; Garavelli, M.; Keseru, G.; Naray-Szabo, G. *Chem. Phys. Lett.* **2002**, *362*, 1.

- (280) Kuno, M.; Palangsuntikul, R.; Hannongbua, S. *J. Chem. Inf. Comput. Sci.* **2003**, *43*, 1584.
- (281) He, X.; Mei, Y.; Xiang, Y.; Zhang da, W.; Zhang, J. Z. *Proteins* **2005**, *61*, 423.
- (282) Mei, Y.; He, X.; Xiang, Y.; Zhang da, W.; Zhang, J. Z. *Proteins* **2005**, *59*, 489.
- (283) Rittenhouse, R. C.; Apostoluk, W. K.; Miller, J. H.; Straatsma, T. P. *Proteins* **2003**, *53*, 667.
- (284) Abashkin, Y. G.; Erickson, J. W.; Burt, S. K. *J. Phys. Chem. B* **2001**, *105*, 287.
- (285) Kumar, D.; Hirao, H.; de Visser, S. P.; Zheng, J.; Dongqi, W.; Thiel, W.; Shaik, S. *J. Phys. Chem. B* **2005**, *109*, 19946.
- (286) Bathelt, C. M.; Zurek, J.; Mulholland, A. J.; Harvey, J. N. *J. Am. Chem. Soc.* **2005**, *127*, 12900.
- (287) Oda, A.; Yamaotsu, N.; Hirono, S. *J. Comput. Chem.* **2005**, *26*, 818.
- (288) Rupp, B.; Raub, S.; Marian, C.; Höljtje, H. D. *J. Comput.-Aided Mol. Des.* **2005**, *19*, 149.
- (289) Favia, A. D.; Cavalli, A.; Masetti, M.; Carotti, A.; Recanatini, M. *Proteins* **2006**, *62*, 1074.
- (290) Hackett, J. C.; Brueggemeier, R. W.; Hadad, C. M. *J. Am. Chem. Soc.* **2005**, *127*, 5224.
- (291) de Visser, S. P.; Kumar, D.; Cohen, S.; Shacham, R.; Shaik, S. *J. Am. Chem. Soc.* **2004**, *126*, 8362.
- (292) Kamachi, T.; Yoshizawa, K. *J. Am. Chem. Soc.* **2003**, *125*, 4652.
- (293) Bathelt, C. M.; Ridder, L.; Mulholland, A. J.; Harvey, J. N. *Org. Biomol. Chem.* **2004**, *2*, 2998.
- (294) Bathelt, C. M.; Ridder, L.; Mulholland, A. J.; Harvey, J. N. *J. Am. Chem. Soc.* **2003**, *125*, 15004.
- (295) Guallar, V.; Baik, M. H.; Lippard, S. J.; Friesner, R. A. *Proc. Natl. Acad. Sci., U.S.A.* **2003**, *100*, 6998.
- (296) Kuhn, B.; Jacobsen, W.; Christians, U.; Benet, L. Z.; Kollman, P. *A. J. Med. Chem.* **2001**, *44*, 2027.
- (297) Humphrey, W.; Dalke, A.; Schulten, K. *J. Mol. Graphics* **1996**, *14*, 33–8, 27–8.

CR050579P